



UNIVERSIDAD DE JAÉN

DOCTORAL THESIS

**Aerodynamic improvement of blunt
bodies through flexible devices**

Author:

Carlos GARCÍA BAENA

Supervisors:

Dr. José Ignacio JIMÉNEZ GONZÁLEZ
Dr. Cándido GUTIÉRREZ MONTES

in the

Grupo de Mecánica de Fluidos e Interacción Fluido-Estructura TEP-235
Departamento de Ingeniería Mecánica y Minera

Jaén, November 27, 2023

DEPARTAMENTO DE INGENIERÍA MECÁNICA Y MINERA
Escuela Politécnica Superior de Jaén

Aerodynamic improvement of blunt bodies through flexible devices

**Mejora aerodinámica de cuerpos romos mediante dispositivos
flexibles**

Autor
Carlos García Baena

Directores de Tesis
Dr. José Ignacio Jiménez González
Dr. Cándido Gutiérrez Montes

Jaén, November 27, 2023

A mis padres, hermano y demás inestimables compañeros de viaje

*A boat beneath a sunny sky
Lingering onward dreamily
In an evening of July—*

*Children three that nestle near,
Eager eye and willing ear,
Pleased a simple tale to hear—*

*Long has pale that sunny sky:
Echoes fade and memories die:
Autumn frosts have slain July.*

*Ever drifting down the stream—
Lingering in the golden gleam—
Life, what is it but a dream?*

— Lewis Carroll, *Through the Looking-Glass
and What Alice Found There*

Tesis Doctoral

AERODYNAMIC IMPORVEMENT OF BLUNT BODIES THROUGH
FLEXIBLE DEVICES

Autor:
Carlos García Baena

Directores de Tesis:
Dr. José Ignacio Jiménez González
Dr. Cándido Gutiérrez Montes

Firma del tribunal Calificador:

Firma

Presidente: Manuel García-Villalba Navaridas
Vocal: Rémi Bourget
Secretaria: Paloma Gutiérrez Castillo
Suplente: Patricia Ern
Suplente: Conrado Ferrera Llera

Calificación:

Jaén, November 27, 2023

Agradecimientos

Al volver la vista atrás apenas puedo ver todo el camino que he recorrido desde que decidí embarcarme en esta ardua pero maravillosa empresa. Han sido tiempos de grandes cambios, tanto en lo profesional como en lo personal, y ahora me toca acordarme de todos los que estuvieron conmigo en unas cuantas líneas. La solitaria mesa, el ordenador legado y el laboratorio rara vez concurrido en el que empecé, ahora difícilmente acoge a las personas que lo habitan, así que intentaré no dejar a nadie en el olvido y agradecer a los muchos que me han ayudado a llegar hasta aquí.

Para empezar, a mis directores de tesis. A José Ignacio, como una fuerza imparable del trabajo que ni la paternidad por partida doble ha conseguido apaciguar, gracias por tirar de mí con una infinita paciencia, siempre con alguna brillante idea en la cabeza cuando estaba perdido y obligarme a tender a la extenuante perfección de la presentación científica que ostentas. A Cándido, por estar siempre dispuesto a un golpe de teléfono, con elaboradas e inteligentes conversaciones y una buena música de fondo, gracias por ser mi mentor en el prelude de mi docencia y por sacarnos de los enredos en los que inevitablemente siempre acabamos, con una sonrisa. A Carlos, como un ejemplo a seguir, tanto en lo académico como en lo personal, gracias por guiarnos por todo este nuevo mundo de investigación, papeles y burocracia, siempre con autoridad, seguridad y una buena cerveza cuando hacía falta. Aunque el exceso de directores y la temática de mis estudios no nos hayan juntado en la investigación, no me puedo olvidar de Rocío y todo lo que me ha ayudado entre prácticas, becas y demás, gracias por recibirme siempre con amabilidad y amenas conversaciones.

Por supuesto, agradecer a los compañeros que me recibieron a mi llegada, Manu y Javi. Dos personas extraordinariamente trabajadoras que no dudaron en acogermme y en echarme una mano a cada problema que encontraba y que me advirtieron, casi a diario, de las tribulaciones del doctorado. Escribiendo esto desde mi encierro entre pantallas, pienso que quizás debí haberlos escuchado con más detenimiento, ahora empiezo a entenderlos un poquito mejor. También agradecer a mis compañeros de armas, más duchos en el café y las charlas que con la espada, Paco, Antonio, Camacho y Fran que han hecho que bajar cada día a la universidad valga la pena solo por estar un rato con ellos, y no podría agradecer más ese altruismo con el que tantas veces me han ayudado. No se me puede olvidar, principalmente a partir de mis inicios con la experimentación (pese al cariño que le proceso a la simulación numérica, esta tiende a ser un camino virtual y solitario cargado de introspección e interminables búsquedas en foros), agradecer enormemente a las hábiles manos ejecutoras de Mario y Arturo, grandes técnicos y personas, que han sabido atender de buena gana mis delirios de ingeniero, que aunque siempre en pos de la ciencia a veces se alejaban un poco de lo ortodoxo.

Conforme escribo, me voy dando cuenta de la cantidad de gente que ha intervenido en mi carrera como doctorando y de que podría hacer unos agradecimientos más grandes que la propia Tesis, pero como ese no es mi objetivo, haré un pequeño resumen. Muchas gracias a la gente de Linares, Mario Miró, Javi Aceituno y Mariano con los que pasé muy buenos ratos y me enseñaron tanto en mi estreno como profesor. También agradecer a la gente del departamento de Ingeniería Mecánica y Minera de Jaén y alrededores, que siempre se han portado tan bien conmigo.

Creo que jamás podré olvidar mi estancia en París, cuando en medio de la pandemia, sin mucha premeditación y con el final de la Tesis pisándome los talones, cogí un avión hacia la capital francesa. Agradecer enormemente a la gente del PMMH, en

especial al grupo BIOMIM por acogerme tan cálidamente a pesar de mi escasa destreza en el francés y sobre todo a Ramiro por ser un excelente anfitrión. En especial quiero agradecer mi estancia a toda la gente del Colegio de España, que destruyeron por completo mi inmersión lingüística, incluso llegándome a hacer pensar que en algún momento de la noche habíamos invadido un pedazo de Francia sin que estos se diesen cuenta, pero a cambio me hicieron pasar unos meses increíbles, tan intensos que se diría que pasé allí una vida.

Para terminar, ya fuera de lo profesional, pero igual o más importante. A mis amigos, ya sean los nuevos que he ido haciendo en este viaje o los incondicionales baezanos diseminados por el mundo. Sobre todo, al de las interminables charlas nocturnas sin discordancia, inmóvil mientras se lía un cigarro al otro lado de la grieta y al imprevisible genio de las palabras, capaz de extenuar lo que se arremolina en la psique con un par de frases. Y por supuesto, a mi pequeña familia, a mis padres que han estado siempre ahí dándome ánimos, deseosos de saber de mí y mis quehaceres y a mi hermano, con el que he podido compartir tantas cosas a lo largo de estos años.

Resumen

El creciente problema del calentamiento global y el incremento del coste de los carburantes y de la electricidad está haciendo plantearse a muchos gobiernos la necesidad de cambiar sus hábitos de consumo energéticos. En particular, la incesante emisión de dióxido de carbono (CO_2) es una de las principales causas del cambio climático, siendo una de las fuentes más importantes de emisión de CO_2 el consumo de gasoil en vehículos de transporte pesados terrestres (autocares, camiones-tráiler, furgonetas, etc.), que es en parte empleado en vencer la fuerza resistente ejercida por el aire.

El estudio de este tipo de vehículos resulta de especial interés, puesto que su forma está diseñada para optimizar la capacidad de carga, transporte de la misma y su descarga, dejando la aerodinámica en un segundo plano. De manera específica, la parte trasera de estos vehículos resulta de gran interés ya que, dada su geometría en forma de corte abrupto, produce un desprendimiento masivo y alternativo del flujo al separarse bruscamente la capa límite, lo que genera una zona de baja presión cerca de la superficie posterior del cuerpo. Esta zona de baja presión es la causante de hasta un cuarto de la resistencia aerodinámica total del vehículo.

La estela generada por estos vehículos se asemeja a la producida por cuerpos romos, razón por la cual existe una gran cantidad de estudios en la bibliografía centrados en el análisis de la estela o las fuerzas aerodinámicas alternativas en este tipo de geometrías simplificadas. En particular, las diferencias de presión entre la parte delantera y trasera del cuerpo inducen una fuerza neta sobre el mismo que se opone al avance del vehículo, por lo que aumentar la presión en la parte posterior del cuerpo ayudaría a disminuir esta fuerza de arrastre. De esta forma, estos estudios buscan controlar la estela tras los cuerpos romos, tanto de forma espacial como temporal, con el objeto de reducir la resistencia aerodinámica y/o estabilizar la estela, con el fin de controlar o atenuar las fuerzas laterales alternativas en el tiempo que también afectan a este tipo de cuerpos.

La cantidad de formas de abordar este problema que podemos encontrar en la literatura es extensa. El presente trabajo se centra en el estudio del uso de cavidades traseras, un tipo de dispositivos pasivos muy estudiados debido a su gran eficacia, que ya se empiezan a utilizar a día de hoy gracias a los cambios en las normativas de tráfico de los distintos países. El fundamento detrás de estas estructuras reside en la separación de la zona de desprendimiento de vortices aguas abajo de la base del cuerpo, aumentando la presión sobre la superficie trasera y reduciendo así la fuerza de arrastre sobre el cuerpo sin ningún tipo de aporte energético externo. El problema de estos dispositivos reside en que su eficacia está ligada a su longitud y forma, haciendo que para conseguir grandes reducciones de la resistencia aerodinámica se necesiten estructuras que son impracticables para poder operar con estos vehículos o para las leyes de tráfico actuales. Además su rendimiento disminuye considerablemente bajo condiciones de flujo cruzado, que constituye una situación muy extendida en aplicaciones reales de vehículos.

Este tipo de cavidades rígidas ha sido ampliamente investigado, por lo que el objetivo de esta Tesis se centrará en el estudio de sistemas optimizados como cavidades formadas por lamina puramente flexibles o lamina rígidas con uniones flexibles, más atractivas a efectos prácticos por simplicidad de implementación y de menor complejidad dinámica. Esta visión del problema nace de una inspiración en la naturaleza,

donde tanto la reconfiguración pasiva de árboles y plantas para reducir su resistencia al viento como el nado de las criaturas acuáticas o el vuelo de aves, mamíferos e insectos está basado en estructuras flexibles. El principal tema de esta Tesis lo ocupa el estudio del problema de interacción fluido-estructura del flujo alrededor de cuerpos de base roma que implementa cavidades de lamas totalmente flexibles, en su primera parte, y lamas rígidas montadas de forma flexible en la segunda. El estudio se realiza considerando distintos números de Reynolds y se aborda tanto de forma numérica, mediante el uso de OpenFOAM, como experimental, usando células de carga para medir las fuerzas, técnicas PIV para caracterizar la estela y sensores láser junto con correlación digital de imágenes para captar el movimiento de las lamas.

En la primera parte de esta disertación, se estudia numéricamente el flujo a bajos números de Reynolds alrededor de un cuerpo de base roma que implementa dos lamas flexibles empotradas en su base. El análisis muestra la existencia de tres regímenes en el comportamiento de la cavidad y la estela en función de la flexibilidad de las lamas. Cuando la frecuencia del desprendimiento de vórtices de la estela y la natural de las lamas coinciden, aparecen oscilaciones de gran amplitud que provocan el aumento de las fuerzas de arrastre pero reducen en gran medida las fuerzas laterales fluctuantes sobre el cuerpo. Por otro lado, cuando la frecuencia de la estela es menor que la natural de las lamas, éstas se mueven de forma antisimétrica, consiguiendo periodos de grandes reducciones de las fuerzas de arrastre y estabilizando la estela, incrementándose esta mejora para mayores amplitudes de la oscilación de las lamas, que se pueden obtener mediante un aumento de la respuesta dinámica de las mismas. En este análisis también se lleva a cabo un estudio para estimar la cantidad de energía que se podría obtener a partir de la deformación y oscilación de las lamas, por ejemplo, transformándola en energía eléctrica mediante materiales piezoeléctricos. Posteriormente, se presenta un estudio experimental del flujo turbulento alrededor de un cuerpo similar más esbelto. El análisis muestra que el uso de este tipo de cavidades presenta una considerable reducción de las fuerzas de arrastre, derivada de una compleja reconfiguración pasiva de las lamas a medida que aumenta su flexibilidad, lo que provoca una disminución del tamaño de la burbuja de recirculación y un mayor aumento asociado de la presión en la base.

En la segunda parte, se considera el uso de sistemas de orden reducido, para lo cual se analizan dispositivos formados por lamas rígidas montadas con rótulas elásticas. De esta forma se consigue simplificar el problema desde el punto de vista dinámico, lo que permite ahondar en el entendimiento de los mecanismos responsables de las mejoras aerodinámicas observadas, así como simplificar la implementación de estos elementos en vehículos a escala real. Primeramente, se lleva a cabo el análisis numérico del flujo a bajos números de Reynolds alrededor de un cuerpo de base roma esbelto 2D, similar al estudiado experimentalmente en la primera parte, con un par de lamas montadas de forma flexible, mediante rótulas torsionales, a la base. Los resultados muestran que este tipo de solución proporciona una reducción de las fuerzas de arrastre pequeña pero tiene un gran potencial para reducir las fuerzas laterales y mejorar el control de la estela. Adicionalmente, se desarrollan técnicas multicuerpo para obtener las fuerzas locales sobre las lamas a partir del movimiento de las mismas. Seguidamente, se aborda el estudio experimental y numérico, a números de Reynolds mayores, de un cuerpo similar con platos rígidos unidos mediante rótulas torsionales elásticas. En el mismo se observan reducciones considerables de las fuerzas de arrastre gracias a la reconfiguración pasiva promedio de las lamas, que aumenta a medida que se reduce la rigidez de las uniones, haciendo la estela más aerodinámica y aumentando la presión en la base. Esta mejora aerodinámica se observa para distintos ángulos de guiñada, lo que extiende la utilidad del sistema a su aplicación en situaciones de flujo real en

carretera, como el flujo cruzado.

Finalmente, como apéndice, se incluyen los resultados preliminares de un estudio experimental sobre las fuerzas y caracterización tridimensional del aleteo de alas flexibles rigidizadas mediante dos venas, e inspirado en el vuelo de insectos. Dicho análisis es presentado como un ejemplo de la aplicación potencial de la metodología experimental utilizada anteriormente a problemas bioinspirados que involucran elementos flexibles.

Los resultados derivados de este trabajo han sido publicados o están en trámites de publicación en los siguientes artículos:

- **C. García-Baena**, J.I. Jiménez-González, C. Gutiérrez-Montes & C. Martínez-Bazán (2021) Numerical analysis of the flow-induced vibrations in the laminar wake behind a blunt body with rear flexible cavities. *Journal of Fluids and Structures*, 100, 10.1016/j.jfluidstructs.2020.103194.
- **J.I. Jiménez-González**, C. García-Baena, J.F. Aceituno & C. Martínez-Bazán (2021) Flow-induced vibrations of a hinged cavity at the rear of a blunt-based body subject to laminar flow. *Journal of Sound and Vibration*, 495, 10.1016/j.jsv.2020.115899.
- **C. García-Baena**, J.I. Jiménez-González & C. Martínez-Bazán (2021) Drag reduction of a blunt body through reconfiguration of rear flexible plates. *Physics of Fluids*, 33, 10.1063/5.0046437.
- **C. García-Baena**, J.M. Camacho-Sánchez, J.I. Jiménez-González, C. Gutiérrez-Montes & C. Martínez-Bazán (2022) Drag improvement on a blunt-base body by self-adaption of rear flexibly hinged flaps. *Enviado a Journal of Fluids and Structures*.
- **C. García-Baena**, R. Godoy-Diana, R. Antier, J.I. Jiménez-González, C. Gutiérrez-Montes & B. Thiria (2022) Insect-inspired two-vein flapping wings with anisotropic rigidity. *En preparación*.

Palabras Clave: Vibraciones inducidas por el flujo, cuerpos romos, elementos pasivos, cavidad trasera flexible, dinámicas multicuerpo, lamas flexibles, control del flujo, interacción fluido-estructura, reducción del drag, recolección de energía, reconfiguración de lamas traseras, alas bio-inspiradas y rigidez anisotrópica.

UNIVERSIDAD DE JAÉN

*Abstract*Escuela Politécnica Superior de Jaén
Departamento de Ingeniería Mecánica y Minera

Doctor of Philosophy

Aerodynamic improvement of blunt bodies through flexible devices

by Carlos GARCÍA BAENA

The problem of global warming and the increase in the cost of energy is driving many governments to revise and optimize their energy consumption habits. The increasing emission of carbon dioxide (CO₂) is one of the main causes of climate change, in which heavy vehicles (buses, trucks, vans, etc.) are a major contributor. In that regard, a great part of the total energy expense in a road vehicle, especially for heavy-duty vehicles, is due to wind aerodynamic resistance or drag force.

The study of these types of vehicles is of special interest, since their shape is designed to maximize the load capacity, and presents poor aerodynamic performance. In particular, the rear part of these vehicles is of great interest, since it is responsible for the massive and alternative detachment of the flow when the boundary layer suddenly separates, which generates a low pressure region close to the base of the body. As a consequence, the rear part of the vehicle or base is known to cause a 25% of the total drag due to the formation of this low-pressure zone.

The wake generated by these vehicles is similar to the one observed in blunt base bodies. In that regard, numerous studies have been conducted focused on the analysis of the wake or the alternative aerodynamic forces in these types of simplified geometries. In particular, pressure differences between the front and rear of the body induce a net force that opposes the vehicle's progress. Thus, increasing the pressure on the rear part of the body would yield an decrease in the drag force. In this way, the control of the wake behind these blunt bodies, both spatially and temporally, has been seen to reduce the aerodynamic drag and/or stabilize the wake.

The present work focuses on the study of the use of rear cavities, a widespread passive control device. The rationale behind these structures lies in the downstream separation of the vortex shedding zone from the base of the body, which causes an increase in the pressure at this area and, thus, a drag reduction without the need of any external energy input. However, the effectiveness of these devices largely depends on their length and shape, and their performance decreases under cross-flow conditions, which significantly hinders their implementation and use in real vehicles as well as reduces their performance and utility.

These types of rigid cavities have been extensively investigated. Therefore, the main aim of the present Thesis is the design of rear optimized devices for passive wake control, capable of adapting passively to changing conditions of the flow. Specifically, the use of rear cavities installed with the addition of flexible junctions or cavities made of flexible plates is proposed and analyzed under different aligned and cross flow conditions. Furthermore, the main subject of this Thesis focuses on the study of the fluid-structure interaction problem of the flow around blunt base bodies that implements, on the one hand, fully flexible plates cavities and, on the other hand, flexibly-mounted rigid plates. The study is carried out considering different Reynolds

numbers and yaw angles. To this aim, numerical simulations, using OpenFOAM, and experimental tests, with the use of force measurements, particle image velocimetry (PIV) or digital image correlation, among others, will be conducted to characterize the problem.

The present dissertation is divided into two different parts. Part 1 considers the use of purely flexible foils or plates in rear cavities as passive control and drag reduction strategies in wakes behind blunt-based bodies. First, the numerical study of a 2D fluid-structure interaction problem of a laminar flow around a D-shaped body implementing two flexible plates forming a cavity at the rear end is addressed. The characterization of the different regimes is conducted considering different values of the non-dimensional stiffness of the plates, focused on the effect on the wake and the aerodynamic forces acting on the body. Furthermore, an energy harvesting analysis of the plates vibrations is also carried out. Additionally, the experimental study of the fluid-interaction problem in the wake of a D-shaped slender body subject to turbulent flow is then presented. Therein, the effect of a rear flexible cavity is assessed, focused on the impact of the shape reconfiguration on the wake, the vortex shedding process and the aerodynamic forces. To that aim laser visualizations, load cell measurements and digital images analysis are conducted to characterize the complex deformations of the plates.

On the other hand, Part 2 analyzes the use of reduced order systems, for which devices formed by flexibly-hinged rigid plates are analyzed. In this way, the problem is simplified, which allows deepening the understanding of the mechanisms responsible for the aerodynamic improvements observed, as well as simplifying the dynamics and implementation of these elements in full-scale vehicles. Therefore, a numerical study of the flow-induced vibrations for a 2D D-shaped slender body implementing a flexibly-hinged cavity and subject to laminar flow is first presented. The plates are mounted with torsional hinges whose stiffness is parametrically varied to evaluate the effect of the reduced velocity on the plates dynamic response and wake features. Furthermore, a multibody model has been developed to retrieve, from the plates rotational motion, the resultant forces and moments produced by the plates vibration. Next, an experimental study is conducted for the aforementioned configuration with flexibly-mounted rear plates, subject to turbulent flow. In particular, the problem is studied with help of laser visualizations and force measurements. The problem is also numerically tackled by performing transient and turbulent simulations to analyze in detail the pressure in the wake and shedding process.

Finally, as an appendix, preliminary results are included on the experimental study of forces and three-dimensional deflection of insect-inspired two-vein flapping wings, as an example of the potential application of the previously used experimental methodology to bio-inspired problems involving flexible elements.

The results of this dissertation have been published or are being submitted in the following journals:

- **C. García-Baena, J.I. Jiménez-González, C. Gutiérrez-Montes & C. Martínez-Bazán** (2021) Numerical analysis of the flow-induced vibrations in the laminar wake behind a blunt body with rear flexible cavities. *Journal of Fluids and Structures*, 100, 10.1016/j.jfluidstructs.2020.103194.
- **J.I. Jiménez-González, C. García-Baena, J.F. Aceituno & C. Martínez-Bazán** (2021) Flow-induced vibrations of a hinged cavity at the rear of a blunt-based

body subject to laminar flow. *Journal of Sound and Vibration*, 495, 10.1016/j.jsv.2020.115899.

- **C. García-Baena**, J.I. Jiménez-González & C. Martínez-Bazán (2021) Drag reduction of a blunt body through reconfiguration of rear flexible plates. *Physics of Fluids*, 33, 10.1063/5.0046437.
- **C. García-Baena**, J.M. Camacho-Sánchez, J.I. Jiménez-González, C. Gutiérrez-Montes & C. Martínez-Bazán (2022) Drag reduction on a blunt body by self-adaption of rear flexibly hinged flaps. *Journal of Fluids and Structures*, 118, 10.1016/j.jfluidstructs.2023.103854.
- **C. García-Baena**, R. Godoy-Diana, R. Antier, J.I. Jiménez-González, C. Gutiérrez-Montes & B. Thiria (2022) Insect-inspired two-vein flapping wings with anisotropic rigidity. *Under preparation*.

Keywords: Flow-induced vibrations, bluff body, passive control, rear flexible cavity, multibody dynamics, flexible plates, flow control, fluid-structure interaction, drag reduction, energy harvesting, rear plates reconfiguration, bio-inspired flapping wings and anisotropic rigidity.

Contents

Agradecimientos	xi
Resumen	xiii
Abstract	xvii
1 Introduction	1
1.1 General context and motivation	1
1.2 Wake dynamics of bluff bodies and simplified road models	3
1.3 Wake control and drag reduction strategies	4
1.3.1 Flexible strategies of wake control and drag reduction	6
1.4 Outline of the dissertation	11
I Rear cavities of flexible plates	13
2 Numerical analysis of wake behind a blunt body with rear flexible plates.	15
3 Drag reduction of a blunt body through reconfiguration of rear flexible plates.	17
II Rear cavities of flexibly-hinged rigid plates	21
4 Numerical analysis of wake behind a blunt body with rear hinged cavity.	23
5 Drag improvement of a blunt base body using rear flexibly hinged flaps	25
6 Conclusions and future work	27
6.1 General conclusions	27
6.2 Future work	31
A Forces and 3D deflection study of insect-inspired two-vein flapping wings	33
A.1 Introduction	33
A.2 Problem description	35
A.3 Experimental set-up	37
A.4 Results	38
A.5 Conclusions and future work	41
Bibliography	43

List of Figures

1.1	Aerodynamic testing at Dryden Flight Research Center to transform an old retired delivery van "shoebox on wheels", in aluminum sheets at 90 degrees, in a vehicle with the minimum fuel consumption and drag coefficient (left). A truck cab over engine tractor trailer, tested and modified to reduce aerodynamic drag (right) [6].	2
1.2	Evolution of mean drag value C_D for road vehicles in the last century [4], [8].	2
1.3	Four key locations for aerodynamics in a trailer truck [10].	3
1.4	Simplified road vehicles models and its geometries. a) Rear devices for aerodynamic drag resistance reduction at real scale trucks [40]. GM or squareback Ahmed, with different aerodynamic drag reduction strategies [9] and c) Ahmed models.	5
1.5	Bluff bodies with fixed rear plates. a) Vorticity fields obtained in laminar numerical simulations of parallel prisms in tandem with a flexible splitter plate [55], b) cylinder with parallel flexible plates [56], c) cylinder with long flexible splitter plate [57] and d) corresponding dynamic response amplitude of a plate for different values of the reduced velocity U^* . e) Experimental work of a prism with a flexible splitter plate in a water channel and an instant view of the wake seeded with particles [58].	7
1.6	Passive reconfiguration: a) relative reduction of the aerodynamic drag coefficient versus the Cauchy number in plants canonical specimens [68], b) progressive deformation of a flexible disk and c) typical evolution of the Vogel exponent γ with the Cauchy number for a flexible plate [39], d) progressive deformation of a flexible plate for an increasing Cauchy number and e) reconfiguration number versus the Cauchy number [73].	10
A.1	The wake behind a rotating wing at low Reynolds number (≈ 500) exhibiting an 'inverted' 'inverted' von Kármán vortex street [92] . . .	36
A.2	(a) and (b) are two examples of different rigidity distribution in insect wings depending on the species [110]. Supporting areas (stippled), deformable areas (unstippled) and flexion lines (dashed) in (a) <i>Syrphus ribesii</i> (Diptera) and (b) <i>Vespulu germunicu</i> (Hymenoptera). median flexion line (m.f.l.), claval furrow (cl.f.) and transverse flexion line (tr.f.l.). Scale lines = 5 mm. (c) Model wing used in the present work. (d) Frontal view of the system mounted on the force sensor with several snapshots superposed to illustrate the flapping wing motion. [115] . .	38
A.3	Set-up of the experiment (a), with the prototype of the printed Zimmerman wing without radial vein (b) and the view from one of the cameras for a 20° radial vein.	39
A.4	Mean force in the advance direction of the model for different angles of the radial vein β and beating frequencies.	39

A.5	Beating cycle for a wing with a $\beta = 10^\circ$ and beating frequency of 13.4 Hz.	40
A.6	Forces in the advance (black) and vertical direction (grey) of the model with each corresponding instantaneous wing deformation a), mean velocity of the leading edge points b) and mean velocity of the trailing edge points c).	40

List of Tables

Chapter 1

Introduction

1.1 General context and motivation

Freight transport industry is all about connections, playing a paramount role in economy and constituting a key factor in globalization, with growing importance in the last years. Although nearly 75% of the world's cargo is transported by sea in large ships, road freight in vehicles, such as trucks or vans, produces 62% of the global freight transport emissions [1], showing a steep increase the last years. According to IEA (2019) [2], energy consumption and CO₂ emissions produced by buses and trucks present a 2.2% growth per year, in a sector dominated by fossil fuel as the main source of energy for road heavy-duty vehicles [3]. Consequently, in recent years the reduction of such greenhouse gas emissions and fuel consumption has been the main goal of new regulations and restrictions in developed countries. In addition, fuel reduction in road freight results beneficial not only in terms of CO₂ and greenhouse gas emissions decrease but also in economic terms stemming from the associated cost reduction of consumed fuel, whose value has been in constant growth in the last years.

Under the above mentioned situation, numerous studies on emissions reduction have been conducted focused on different aspects of the vehicle, such as the development of new engines, optimized mechanics, lighter materials or new more environmentally friendly fuels, among others. A major role is however played by the aerodynamic forces that the heavy-duty vehicles experiment on the road, especially the drag force, i.e. the force acting opposite to the relative motion of the vehicle moving with respect to the surrounding air. The drag force for road vehicles is defined as [4]:

$$f_x = \frac{1}{2} \rho_f c_x A u_{res}^2 \quad (1.1)$$

$$u_{res} = \sqrt{u_\infty^2 + u_{wind}^2 + 2u_\infty u_{wind} \cos(\beta)} \quad (1.2)$$

where ρ_f is the air density, c_x the drag coefficient associated to the vehicle shape, A the effective area of the vehicle, u_∞ the vehicle velocity relative to the road, u_{wind} the wind velocity and u_{res} the velocity magnitude of the vector resulting from the sum of the wind and vehicle velocity with relative yaw angle β . From equation 1.1, the drag aerodynamic force presents a quadratic dependence on the velocity, the latter being of significant importance in highway transport, where the velocities become larger. In this regard, it is estimated that approximately 50% of the total power in a passengers car is invested to overcome the aerodynamic drag [5] in a highway. In the case of heavy duty vehicles, such as trucks, the force and corresponding power required to overcome them, become even larger, since they present larger c_x stemming from their poor aerodynamics, Fig: 1.1.

The large size and the need to maximize the load capacity of heavy vehicles, lead to a decrease in the vehicle aerodynamics, which normally present a big blunt frontal

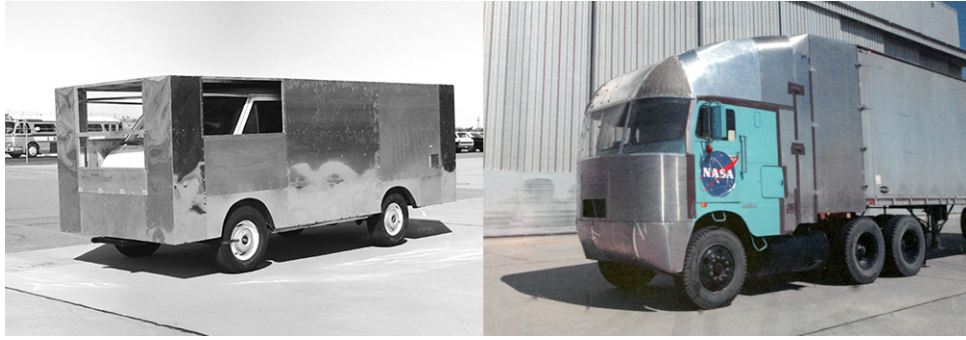


Figure 1.1: Aerodynamic testing at Dryden Flight Research Center to transform an old retired delivery van "shoebox on wheels", in aluminum sheets at 90 degrees, in a vehicle with the minimum fuel consumption and drag coefficient (left). A truck cab over engine tractor trailer, tested and modified to reduce aerodynamic drag (right) [6].

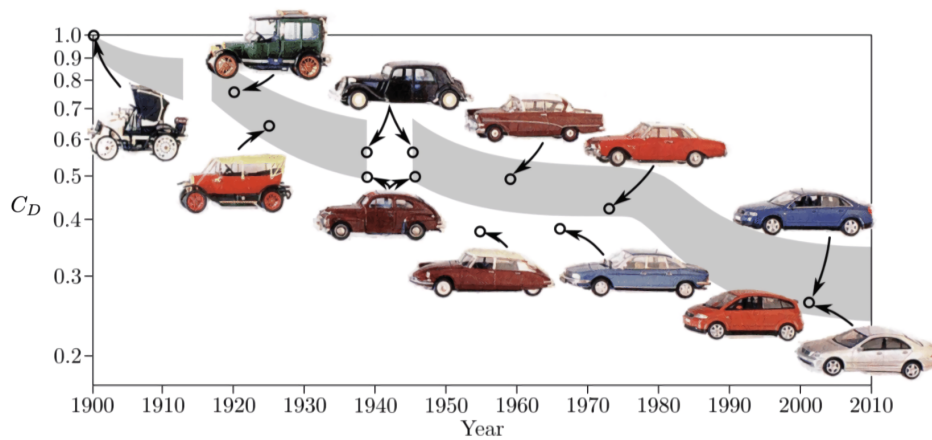


Figure 1.2: Evolution of mean drag value C_D for road vehicles in the last century [4], [8].

surface, with high pressure regions. At the rear part of the truck, a massive flow separation occurs, caused by the abrupt and sharp edges at the end of the trailer box, creating a low pressure zone featuring the development of an intense wake and vortex shedding. The pressure difference between the front and the rear part of the vehicle induces a net force opposed to the truck movement, this being the main contribution to the aerodynamic drag. Other contribution to the aerodynamic resistance is that relative to the viscous forces acting on the vehicle. These forces are produced by the friction of the fluid and the vehicle surface, which are of special importance in low Reynolds number applications or in streamlined bodies such as aircrafts, ships or airfoils [7]. However, in the cases with massive flow separation, such as in road vehicles, it becomes negligible compared to the pressure drag.

In the last century, numerous studies have been conducted to reduce the aerodynamic forces in road vehicles. In particular, the vehicle shape (Fig: 1.2) has been significantly modified towards more optimized, aerodynamic ones. In this regard, trucks, vans or even buses present a lesser evolution, thus, nowadays still presenting less aerodynamic, less efficient shapes, mainly due to load requirements. In addition, the current traffic regulations result even more restrictive for the heavy-duty vehicles, specially in Europe, which makes it more difficult to change the shape of the cab in the case of the trailer trucks, for example. All of the above cause that blunt-based vehicles present a significant potential for improving their aerodynamic performance [9].



Figure 1.3: Four key locations for aerodynamics in a trailer truck [10].

As it can be seen in Fig: 1.3, there are four main regions of a trailer truck that present the greatest potential for aerodynamic drag improvement, namely, the cab front, where the high pressures contribute approximately 25% to the drag force, the gap between the cab and the trailer, where the flow is momentarily detached and constitutes 20% of the drag, the underside, including the wheels, representing 30% of the force, and the rear of the trailer with a massive detachment of the flow and vortex shedding, which constitutes 25% of the resistance force [10], [11]. The rear part of the trailer is one of the less studied regions, or optimized for that matter, in terms of aerodynamic performance. Therefore, the present work is focused on this part. In particular, the main aim is the design of different devices, for passive wake control, implemented at the rear part of the body, specifically rear cavities installed with the addition of flexible junctions or cavities made of flexible plates used in reducing the drag coefficient under different scenarios, which include cross flow or transient flow configurations.

1.2 Wake dynamics of bluff bodies and simplified road models

The flow around bluff bodies is a classic problem in the field of fluid mechanics, both for laminar and turbulent regimes. Both regimes present common features, what allows the design and extrapolation of global control strategies or results from modal analysis in laminar wakes to turbulent flows. Some examples that support this hypothesis can be found in the effectiveness of similar passive structures used for flow stabilization in laminar wakes ([12], [13]) and turbulent ones ([14]–[16]). Therefore, numerous studies on aerodynamic drag reduction in laminar wakes have been proven effective in turbulent regimes, including different passive devices such as spoilers or rear cavities for diverse shapes and depths [17]–[21]. These works also show a clear relation between the aerodynamic improvement and the global stability of the flow. Hence, an improvement of the aerodynamic drag is only possible by means of a deep knowledge of the flow stability.

The analysis of these kinds of problems, such as the flow around a road heavy-vehicle, in a real case scenario using complex geometries and high Reynolds numbers are truly complex problems, either experimentally or numerically [22]–[24]. For this reason, in a first approximation, studies with simplified, scaled models of heavy-duty road vehicles are common, being the Ahmed body [25] one of the most studied and accepted models. Furthermore, the use of 2D simpler models such as a D-shaped cylinder [15], [26]–[29], widely studied in the present dissertation, has been also proven valid and valuable. All these slender models present a rounded front part to prevent flow separation. The flow around these models forms a boundary layer that evolves

longitudinally towards the rear part, where the flow abruptly detaches at the sharp edges generating a strong wake, similar to what can be seen in real road heavy-duty vehicles. The key dimensionless parameter in the definition of the flow regime, is the Reynolds number, defined as:

$$Re = \frac{\rho_f u_\infty h}{\mu_f} \quad (1.3)$$

where u_∞ is the flow velocity, h the model high, ρ_f the density of the fluid and μ_f is the fluid dynamic viscosity. The typical Reynolds numbers in real and industrial applications are of order $O(10^6)$. In scaled model lab experiments for turbulent flows the typical Re values are an order of magnitude lower i.e. $O(10^5)$, but the flow retain the main features of real flows. Therefore, these types of simplified models have been extensively used to evaluate different devices to reduce the aerodynamic drag [30] and subsequently extrapolate the results to real heavy-duty vehicles.

The massive flow detachment occurring at the rear part of the models produces large flow recirculation zones behind the body, that are associated to a pressure drop at the rear part of the body. This low pressure is responsible to a great extent of the aerodynamic drag force F_x and, thus, of its dimensionless coefficient C_x . In that regard, any change of the pressure distribution in the recirculation zone will consequently induce a modification in the aerodynamic of the body and the drag coefficient C_x . Moreover, the abrupt separation of the boundary layer and the wake creation lead to the classic phenomenon of alternative vortex shedding and the induction of oscillatory lateral forces on the body. These effects lead to noise and structural vibrations, whose control is of special importance in some engineering applications. The mitigation of such fluctuating forces and the reduction of the aerodynamic drag have been the goal of many studies, which have led to a large number of different strategies of flow control. Among other passive alternatives, it has been proven that the implementation of rigid rear plates in bluff bodies [31] markedly weakens the amplitude of the fluctuating forces and in some cases the aerodynamic drag, thus, making these types of devices really appealing for practical applications. The latter can be explained by the high sensitivity of the recirculation zone in terms of global stability, since small modifications of the flow can yield the control or the stabilization of the wake perturbations [20], [32], [33]. Both the front and the rear part of these bodies are sensible zones in reducing the aerodynamic drag, but all the restrictions imposed by traffic policies to the cabin of heavy-duty vehicles make the rear zone more appealing in terms of aerodynamic improvement. Nowadays, the latter becomes more relevant in Europe since the new European regulation EU 2015/719 is focused on promoting aerodynamic improvements in trucks that allow the use of mobile and retractable rear control devices.

1.3 Wake control and drag reduction strategies

Wake control strategies to reduce the aerodynamic drag acting on the flow dynamics at the rear end of vehicles can be divided into active or passive ones, based on whether an external source of energy is required or not [9], [34]. The latter mainly consists of the implementation of devices at the rear part of the vehicle to modify the flow topology and improve the aerodynamic performance, such as rigid cavities, spoilers or vortex generators, among others. Nevertheless, the design of these devices is usually based on global flow studies instead of specific optimization methodologies that take

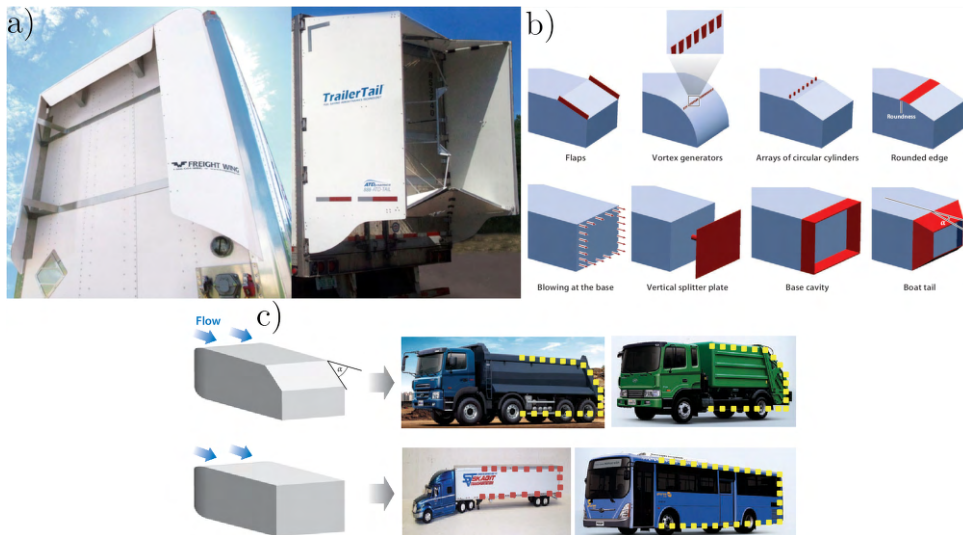


Figure 1.4: Simplified road vehicles models and its geometries. a) Rear devices for aerodynamic drag resistance reduction at real scale trucks [40]. GM or squareback Ahmed, with different aerodynamic drag reduction strategies [9] and c) Ahmed models.

into account the fluid-structure interaction (FSI), what limits their suitability for different scenarios and applications.

The use of flexible devices could present advantages over rigid ones, since the latter are unable to perform optimally in all possible flow conditions [21], and their efficiency significantly decreases in cross flow configurations, very common in real road freight transport. The use of flexible structures could be a more appealing option given their ability to adapt to the flow conditions and modify the rear part of the body to a more aerodynamic shape through passive reconfiguration [35]. This process is widely observed in nature, for example, in plants and trees [36], [37], where the reconfiguration of flexible parts, e.g. leaves, reduce the aerodynamic resistance and the effective area [38]. However, the passive reconfiguration of flexible systems has been scarcely studied in bluff bodies. In this process, the material selection is of great importance [39]. In particular, mechanical properties, such as the flexural rigidity EI , where E is the Young's modulus and I is the moment of inertia with respect to the bending axis, have to be carefully chosen.

The important role of the wake in the aerodynamic forces acting on bluff bodies has led to the design of different devices intended to increase the pressure at the base. Fig: 1.4 shows some of the most studied rigid strategies, such as flaps, base blowing, rounded edges or rear cavities. Some of these strategies are based on the modification of the size of the wake recirculation bubble, where a length increase is directly related to drag reduction [41]. For example, the use of rear cavities [17], [30], [42] has been found to induce a displacement of the low pressure zone downstream, increasing the pressure at the base of the body and, thus, reducing the aerodynamic drag. There is also evidence that these types of structures, regardless of the geometry of the body, can considerably weaken the magnitude of the oscillating forces in the near wake, modifying the boundary layer detachment and displacing the vortex shedding downstream. These effects result in the attenuation of the lateral forces oscillations, what might reduce the risk of flow induced vibrations (FIV) in slender bodies [43], or improve the stability and maneuverability, for example, in applications of heavy-duty transport (Fig: 1.4a), where 3D bluff bodies are involved [40]. Nevertheless, the performance of rigid rear cavities at improving the aerodynamics of a vehicle is

limited by the cavity size [44], a limiting factor in practical applications, where the dimensions of the vehicles are restrained by traffic regulations.

The aforementioned flow control strategies are based on rigid devices of simple geometries or flow modifications supported by a better understanding of the wake. However, they are far from an optimal aerodynamic performance. In that regard, analysis employing gradient methods based on adjoint equations (Lagrangian optimization problems), along with topological algorithms, allow the generation of complete sensibility maps that predict the aerodynamic drag reduction considering different types of geometrical modifications [45] and located perturbations. Thus, the use of optimization tools with adjoint equations [46] and topological algorithms (based on solidly tested free and commercial software) might provide improvement of the previous aerodynamic strategies.

Nevertheless, the effectiveness of rigid passive devices is known to significantly decrease under flow regimes that differ from those they were designed for, such as cross flow configurations. In particular, the presence of cross flow alters flow detachment and the properties of the near wake, increasing the drag and lateral aerodynamic forces, as well as the instabilities of the vehicle [5]. On average, road vehicles circulate most of the time under wind conditions not aligned with the road and, consequently, it is usual to evaluate forces and flow conditions in simplified models considering yaw angles β , which account for misalignment between the model and the incident flow, as considered in eq. (1.2). Typical studies of cross flow analyze the yaw angle in the range of $\beta \leq 10$, meaningful in real road vehicles [5], [47], [48], and in agreement with the vehicle tests designed by the European Union. Therefore, it is common to find experimental and numerical works that analyze the effect of the yaw angle β in the aerodynamic resistance. However, only few of them focus on the effect of the yaw angle on rigid passive control devices, with the exception of some recent works [21], [49]–[51]. In particular, these studies have demonstrated that, in some cases, the performance of rigid devices, such as rear cavities or spoilers, present a total loss of the aerodynamic improvement that they provide when the flow is aligned with the vehicle, what makes them not suitable for a real case scenario on the road, where cross flow is common.

1.3.1 Flexible strategies of wake control and drag reduction

A new approach to flow control and aerodynamic drag reduction arises from the use of flexible structures, whose vibratory dynamics can be used to alter the flow in a similar manner to what is achieved with optimal perturbations and modify the aerodynamic forces on the body. This method, with great potential, has been scarcely studied, and only few studies analyzing the effect of solid deformation and flow stability behind bluff bodies can be found in the literature.

Furthermore, the vibratory dynamics of the flexible flow control elements can also be exploited for energy harvesting, through the use of elements made of piezoelectric materials, regardless of whether they are ceramic, polymeric or composite [52]. In this way, extracting energy from flow induced vibrations (FIV) to charge auxiliary batteries, supply electricity to auxiliary systems of the vehicle or even energy recovery systems for electric vehicles in the future, could be an opportunity to improve transport efficiency. In particular, the basis of this process consists in optimizing the dynamic response of flexible embedded elements or rigid ones implementing flexible joints, taking advantage of vibrational synchronization regimes to maximise deformations [53]. To that aim, a proper characterization of the fluid-structure interaction

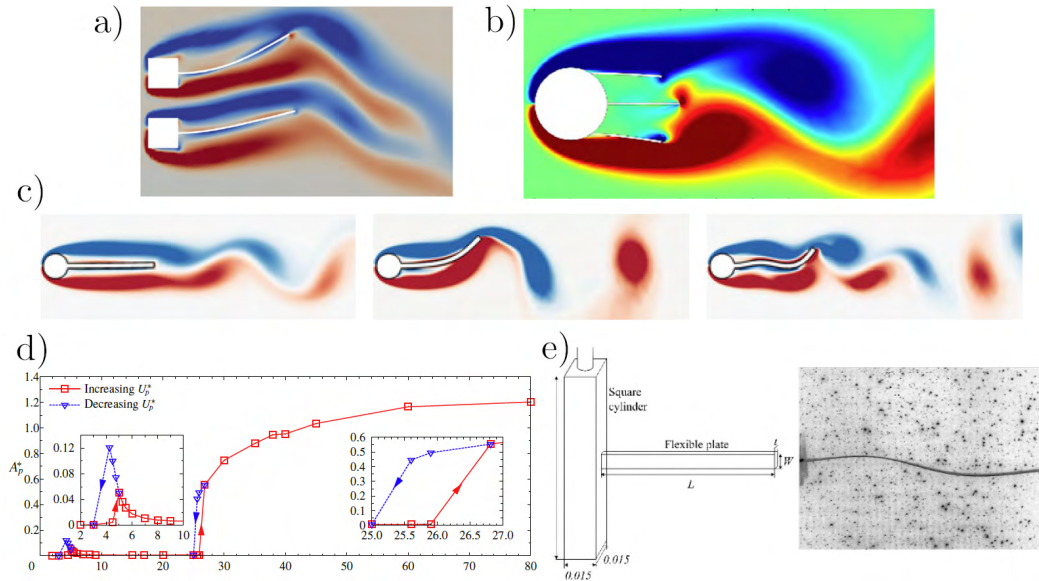


Figure 1.5: Bluff bodies with fixed rear plates. a) Vorticity fields obtained in laminar numerical simulations of parallel prisms in tandem with a flexible splitter plate [55], b) cylinder with parallel flexible plates [56], c) cylinder with long flexible splitter plate [57] and d) corresponding dynamic response amplitude of a plate for different values of the reduced velocity U^* . e) Experimental work of a prism with a flexible splitter plate in a water channel and an instant view of the wake seeded with particles [58].

response results paramount, also considering variations of the reduced velocity U^*

$$U^* = \frac{u_\infty}{f_n h} \quad (1.4)$$

defined as the ratio between the characteristic velocity of the flow u_∞ and that of the vibration $f_n h$, where f_n is the natural frequency of vibration in air of the solid or flexible junction and h is the characteristic height of the body. The use of these systems can generate voltages of order $O(10^1 - 10^2)$ V for piezoelectric areas of $O(10^{-3})$ m^2 [54]. However, the implementation of these systems in road transport has not happened yet. Thus, a good characterization of the energetic potential of the wake behind bluff bodies could represent an important advance to the exploitation of aeroelastic phenomena in external flows with industrial applications.

Besides, the aforementioned performance limitations of passive rigid devices lead to the development of new devices for flow control able to adapt to different flow conditions, in line with the new aerodynamic requirements defined by different institutions, such as those proposed by the European Union. In this way, the use of flexible components constitutes a valid alternative to improve the flow control potential of rear passive systems, whose dimensions are occasionally restricted, and to enhance the energetic balance of vehicles. This approach considers first the exploitation of the vibration dynamics to weaken the vortex shedding in the wake, and reduce the effect of the flow in the body, by means of perturbation of the wake at frequencies different from the essential ones. In this regard, both the flow induced vibrations (FIV) and the flutter (solid vibration to its natural frequency by energy supplied from the flow), disturb and regularize the wake, weakening or inhibiting the shedding of vortices, thus, altering the flow dynamics near the rear zone of the body, sensitive to aerodynamic improvements.

Recent evidences show the potential of using flexible materials for aerodynamic

improvement, whose movement is induced by the fluid-structure interaction. For example, [59] found an important reduction of the aerodynamic drag by adding a flexible fuselage appendage at the rear part of a cylinder, observing that the structural vibrations promote the stabilization of the symmetry breaking of the wake for certain values of the stiffness module EI . The flexural rigidity modifies the natural frequency of the structure f_n , favouring the breaking of the coherent vortex structure when the plates oscillations frequency is decoupled from that of the flow detachment at the wake. The weakening of the principal mode of the wake would provide, in the case of road vehicles, an aerodynamic improvement in terms of periodic undesirable lateral forces. Despite the potential benefits of this approach, the use of flexible systems for flow control in wakes and aerodynamic improvement has been barely applied to bluff bodies and simplified road heavy-duty vehicle models, although the study of the coupled dynamics of the wake in simple 2D bluff bodies with rear flexible plates has attracted the attention of many researchers. For example, the numeric and experimental works on the wake behind a cylinder [55], [60], [61], or a prism of square section [62]–[64] implementing a flexible rear plate have shown a great potential to alter the process of vortex shedding and modify the forces distribution (see Fig: 1.5).

In particular, large modifications of the flow have been found for big amplitudes of the plates oscillations, specially when the vibrations frequencies are close to the first mode of the natural frequency of the flexible structure. In addition, it has been demonstrated that the use of a splitter plate effectively reduces the flow-induced vibrations of cylinders elastically mounted [65]. However, despite the practical relevance in terms of wake control, and unlike the single flexible plate configurations, there are only few works that explore the use of flexible cavities in the rear part of bluff bodies. In this sense, the recent work [56] on the wake behind a cylinder with parallel flexible plates (Fig: 1.5b), reports important reductions of the aerodynamic drag and the magnitude of the lift coefficient, for a particular range of azimuthal angles in the positioning of the rear plates.

In general, these studies have shown that the amplitude of the flow induced vibrations, which characteristic flow velocity is u_∞ , depends on the reduced velocity U^* (eq. 1.4). In particular, for low values of U^* the amplitude of the vibrations is small, due to the plates tend to oscillate with a frequency f_p similar to the one of the flow vortex shedding, f_v . For intermediate values, synchronization phenomena of the coupled problem occurs for the first mode of vibration, so that the ratio between frequencies $f^* = f_p/f_{n,1} \simeq 1$, which considerably amplifies the response and, therefore, the wake perturbations. For high values of U^* , other secondary modes of vibration with higher frequencies are usually excited, increasing the amplitude of the plates oscillation (see Fig: 1.5c,d).

Hence, a proper design of wake perturbation systems through flexible devices, require a thorough previous characterization of the dynamic response and the regimes of the fluid-structure interaction problem. In this sense, the numerical study would be circumscribed to laminar and low Reynolds turbulent regimes for a wide and extrapolated U^* range, due to the limitations of time and computational cost associated to the coupled problem. Thus, the problem characterization of more realistic and turbulent regimes should be carried out experimentally, where the use of high speed cameras and digital image processing could provide the deformation of the plates and the flow in the near wake, also allowing the identification of the different regimes (Fig: 1.5e).

In addition to the reduction of wake fluctuations, flexible systems can also provide an aerodynamic improvement in bluff body vehicles through flow adaptation stemming from passive reconfiguration processes. As previously mentioned, passive

devices are simple, although do not necessarily offer optimal solutions for different flow conditions [34]. Therefore, in the search for simple solutions with ample adaptability to flow, numerous attempts have been made to reproduce or develop bio-inspired flow control strategies based on animals [66], [67] or plants [68]. Of particular interest are the examples of self-adaptive mobile rigid flaps applied to improve the aerodynamic performance of bluff bodies [69]–[71]. In these cases, the quasi-static reconfiguration of the flaps introduce a pressure recovery in the near wake delaying the flow detachment. Similarly, considerable aerodynamic drag reductions can be also achieved by means of passive reconfiguration of the flexible parts, as it happens in plants or trees [36], [37] (Fig: 1.6a). In particular, the observations made by Vogel [38], [72] demonstrated that the deformation of some parts of the plants lead to lower values of aerodynamic drag force F_x , and obtained the relation between the aerodynamic drag and the velocity $F_x \propto u_\infty^{2+\gamma}$, where γ is a negative exponent. In particular, the relative variation of the aerodynamic drag force or the dimensionless drag coefficient defined by the reconfiguration number $\Re = F_x/F_{x,ref} = C_x/C_{x,ref}$, being $F_{x,ref}$ and $C_{x,ref}$ the respective values of the aerodynamic drag force and coefficient for the rigid case without deformation, can reach values ranged 0.05-0.1 for some extreme reconfiguration processes in plants.

The reconfiguration of flexible structures has been widely used in applications of thin films and filaments placed crosswise to the flow stream [35], [39], [74]–[78], where the aerodynamic drag reduction is associated to the shape modification of the bodies, increasing their slenderness, reducing the effective area (Fig: 1.6b,d) and therefore the reconfiguration number (Fig: 1.6e). Recent analysis [73], [79] have shown the existence of certain limits in the adaptability of these flexible structures, associated to regimes of large amplitude oscillations that take place for low Cauchy number, that quantifies the dimensionless stiffness [39]. This dimensionless parameter is defined for flexible elements of length l_p and inertia I , as

$$Ca = \frac{\rho_f u_\infty^2 l_p^3}{2EI} \quad (1.5)$$

and represents the relation between the force produced by the characteristic pressure of the flow (of density ρ_f and velocity u_∞) and the plates stiffness given by EI . Therefore, it is common to observe asymptotic limits in the Vogel exponent $\gamma = 2(\partial \ln \Re / \partial \ln Ca)$ evolution for Cauchy numbers of order $O(10^2 - 10^3)$ (Fig: 1.6c). Therefore, the use of flexible devices able to adapt to different flow conditions constitutes an alternative of great interest when quasi-static reconfigurations are searched in bluff bodies, which occur for low Cauchy numbers Ca . In industrial applications this could be achieved by modifying the material or the dimensions of the plates. Furthermore, the complex dynamics of flexible structural elements, and subsequently of the wake behind the body, has led to numerous studies on the use of moving rigid parts, used as flow and forces control strategies, mounted freely or elastically, since they present simpler dynamics. In some cases these systems can be characterized as a one degree of freedom rigid body. For example, in the context of VIV (vortex induced vibrations) control, [80] showed that placing an individual plate or two plates symmetrically disposed with free or flexible rotation in the rear part of a cylinder reduces considerably the aerodynamic drag due to a near wake and vortex shedding process modification. On the other hand, [81] analyzed the effect of individual rotatory plates of increasing length placed behind of a fixed cylinder, observing aerodynamic drag reductions close to 30% when they oscillate around an angular equilibrium position. The aforementioned improvement was associated to the decoupling between the two

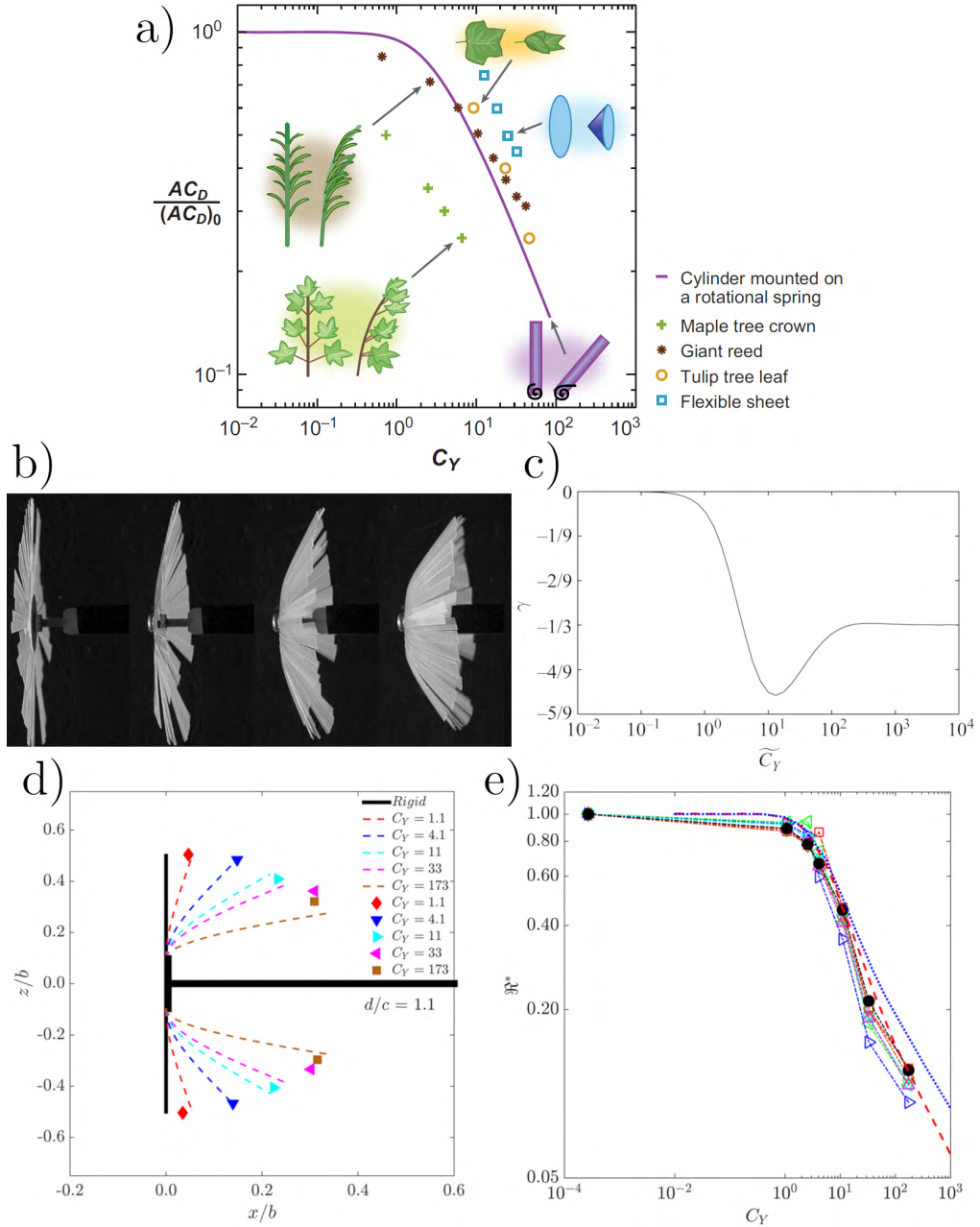


Figure 1.6: Passive reconfiguration: a) relative reduction of the aerodynamic drag coefficient versus the Cauchy number in plants canonical specimens [68], b) progressive deformation of a flexible disk and c) typical evolution of the Vogel exponent γ with the Cauchy number for a flexible plate [39], d) progressive deformation of a flexible plate for an increasing Cauchy number and e) reconfiguration number versus the Cauchy number [73].

shear layers generated at both sides of the cylinder. Similarly, [82] investigated the effect of mobile rigid plates implemented at the laterals of a square cylinder, observing aerodynamic drag reductions up to 22% when the oscillation of the plates altered the dominant frequency of the wake. In general, the efficacy of these passive devices is increased when they are located within the high sensitivity regions to localized perturbations [83], and its potential as a flow control technique in wakes results high given the rupture of unstable modes and their effect in the thrust. In addition, these flexibly mounted systems result in devices whose fluid-structure interaction dynamics can be easily modelled using low order models, as a consequence of the existence of finite number of degrees of freedom [84]. This approach will be also analyzed in the present dissertation to design simple adaptive control devices.

1.4 Outline of the dissertation

The present dissertation is divided into two different parts. Part 1 considers the use of purely flexible foils or plates in rear cavities as passive control and drag reduction strategies in wakes behind blunt-based bodies. First, Chapter 2 presents the numerical study of a 2D fluid-structure interaction problem of a laminar flow around a D-shaped body implementing two flexible plates forming a cavity at the rear end. The characterization of the different regimes is conducted considering different values of the non-dimensional stiffness of the plates, focused on the effect on the wake and the aerodynamic forces acting on the body. Furthermore, an energy harvesting analysis of the plates vibrations is also carried out. Additionally, Chapter 3 includes the experimental study of the fluid-interaction problem in the wake of a D-shaped slender body subject to turbulent flow. Therein, the effect of a rear flexible cavity is assessed, focused on the impact of the shape reconfiguration on the wake, the vortex shedding process and the aerodynamic forces. To that aim laser visualizations, load cell measurements and digital images analysis are conducted to characterize the complex deformations of the plates.

On the other hand, Part 2 analyzes the use of rear cavities of flexibly-mounted rigid plates as passive control devices in wakes behind blunt-based bodies. Chapter 4 presents a numerical study of the flow-induced vibrations for a 2D D-shaped slender body implementing a flexibly-hinged cavity and subject to laminar flow. The plates are mounted with torsional hinges whose stiffness is parametrically varied to evaluate effect of the reduced velocity on the plates dynamic response and wake features. Furthermore, a multibody model has been developed to retrieve, from the plates rotational motion, the resultant forces and moments produced by the plates vibration. Next, Chapter 5 presents an experimental study of the aforementioned configuration with flexibly-mounted rear plates, subject to turbulent flow. In particular, the problem is studied with help of laser visualizations and force measurements. Similar to Chapter 4, the problem is also numerically studied by performing transient and turbulent simulations to analyze in detail the pressure in the wake and shedding process. Chapter 6 collects the main conclusions of this dissertation along with some ideas for future works.

Finally, Appendix A presents preliminary results on the experimental study of forces and three-dimensional deflection of insect-inspired two-vein flapping wings, as an example of the potential application of the previously used experimental methodology to bio-inspired problems involving flexible elements.

Part I

Rear cavities of flexible plates

Chapter 2

**Numerical analysis of wake
behind a blunt body with rear
flexible plates.**



Numerical analysis of the flow-induced vibrations in the laminar wake behind a blunt body with rear flexible cavities



C. García-Baena^{a,b}, J.I. Jiménez-González^{a,b,*}, C. Gutiérrez-Montes^{a,b},
C. Martínez-Bazán^{a,b,c}

^a Departamento de Ingeniería Mecánica y Minera, Universidad de Jaén, Campus de las Lagunillas, 23071, Jaén, Spain

^b Andalusian Institute for Earth System Research, Universidad de Jaén, Campus de las Lagunillas, 23071, Jaén, Spain

^c Departamento de Mecánica de Estructuras e Ingeniería Hidráulica, Universidad de Granada, Campus Fuentenueva s/n, 18071, Granada, Spain

ARTICLE INFO

Article history:

Received 9 July 2020

Received in revised form 30 October 2020

Accepted 12 November 2020

Available online 21 November 2020

Keywords:

Flow-induced vibrations

Blunt-based body

Flexible plates

Flow control

ABSTRACT

We present a numerical study on the fluid–structure interaction of an incompressible laminar flow around a slender blunt-based body implementing a rear cavity of flexible plates. The study focuses on the use of this type of device to control the wake dynamics and the aerodynamic forces acting on the body, as well as to harvest energy from the flow. To that aim, the effects on the plates flow-induced vibrations (FIV) and on the dynamics of the flow of three control parameters, namely the reduced velocity, $0 \leq U^* < 12$, the mass ratio, $m^* = [500, 1000]$ and the cavity height h_c , are evaluated at Reynolds number $Re = 500$. Four different branches are identified in terms of dynamic response, as U^* increases, regardless of the values of h_c and m^* . At low values of U^* , an initial branch with a local peak of moderate amplitude response is observed, where the plates oscillate in counter-phase, in a varicose mode, with a frequency f_p that is synchronized with the second harmonic of the vortex shedding frequency, $2f_{vs}$, and similar to the natural frequency of the solid, $f_n \simeq f_{1,n}$. For intermediate values of U^* , a transition towards a sinuous mode of oscillation occurs, where the plate frequency is synchronized with the vortex shedding frequency, $f_p = f_{vs}$. Initially, after such transition, the oscillation frequency is lower than the natural frequency of the plates $f_p < f_{1,n}$, so that a weak response defines a lower branch in the amplitude response curve. When U^* increases, a lock-in regime develops with $f_p = f_{vs} = f_{1,n}$, that is characterized by a response amplification, giving rise to the emergence of the upper branch, where the FIV amplitude of plates is the highest. Finally, a fourth desynchronization branch of moderate amplitude appears for larger values of U^* , where the plates present a complex, multi-mode regime, characterized by the vibration at multiple frequencies within the range $5f_{1,n} < f_p < 6.5f_{1,n}$. The analysis of the plates deformation through POD analysis reveals that they mainly oscillate following the first Euler–Bernoulli mode for the first three branches, and a combination of the second and first Euler–Bernoulli modes for the desynchronization branch. The effect of increasing the mass ratio is to mitigate the response at higher values of U^* , while reducing the cavity height h_c leads to the fostering of oscillations within the upper and desynchronization branches. In general, the FIV response of plates alters the wake dynamics and the force coefficient, especially within the lock-in regime, where the drag is strongly amplified, although the fluctuations of the lift are attenuated (nearly a 40% reduction). Besides, reductions of the drag of approximately 2% are obtained within the initial and lower branches. Finally, a simple quantification of the energy transfer from the plates, through a linearized Euler–Bernoulli

* Corresponding author at: Departamento de Ingeniería Mecánica y Minera, Universidad de Jaén, Campus de las Lagunillas, 23071, Jaén, Spain.
E-mail address: jignacio@ujaen.es (J.I. Jiménez-González).

Chapter 3

Drag reduction of a blunt body through reconfiguration of rear flexible plates.

Drag reduction of a blunt body through reconfiguration of rear flexible plates

Cite as: Phys. Fluids **33**, 045102 (2021); <https://doi.org/10.1063/5.0046437>

Submitted: 03 February 2021 . Accepted: 10 March 2021 . Published Online: 01 April 2021

 C. García-Baena,  J. I. Jiménez-González, and  C. Martínez-Bazán



View Online



Export Citation



CrossMark

ARTICLES YOU MAY BE INTERESTED IN

[Active flow control of the dynamic wake behind a square cylinder using combined jets at the front and rear stagnation points](#)

Physics of Fluids **33**, 047101 (2021); <https://doi.org/10.1063/5.0043191>

[Flow-induced vibrations of a pair of in-line square cylinders](#)

Physics of Fluids **33**, 043602 (2021); <https://doi.org/10.1063/5.0038714>

[The scales of the leading-edge separation bubble](#)

Physics of Fluids **33**, 045101 (2021); <https://doi.org/10.1063/5.0045204>

Physics of Fluids

SPECIAL TOPIC: Tribute to
Frank M. White on his 88th Anniversary

SUBMIT TODAY!



Drag reduction of a blunt body through reconfiguration of rear flexible plates

Cite as: Phys. Fluids **33**, 045102 (2021); doi: [10.1063/5.0046437](https://doi.org/10.1063/5.0046437)

Submitted: 3 February 2021 · Accepted: 10 March 2021 ·

Published Online: 1 April 2021



View Online



Export Citation



CrossMark

C. García-Baena,^{1,2}  J. I. Jiménez-González,^{1,2,a)}  and C. Martínez-Bazán^{1,2,3} 

AFFILIATIONS

¹Departamento de Ingeniería Mecánica y Minera, Universidad de Jaén, Campus de las Lagunillas, 23071 Jaén, Spain

²Andalusian Institute for Earth System Research, Universidad de Jaén, Campus de las Lagunillas, 23071 Jaén, Spain

³Departamento de Mecánica de Estructuras e Ingeniería Hidráulica, Universidad de Granada, Campus Fuentenueva s/n, 18071 Granada, Spain

a) Author to whom correspondence should be addressed: jignacio@ujaen.es

ABSTRACT

We investigate the quasi-static reconfiguration of rear parallel flexible plates on the drag coefficient of a blunt body. The drag coefficient, plates deformation, and main features of the turbulent wake are characterized experimentally in a towing tank. It is found that increasing the flexibility of plates leads to an important drag reduction, induced by the progressive streamlining of the trailing edge due to plates deformation. The study of the Vogel exponent is adopted here to evaluate the limit on the potential drag reduction at large values of the Cauchy number, which is shown to be mainly caused by the growth in the vibrating amplitude response of plates. The plates deformation is analyzed by means of image processing, showing that their shapes mainly follow the first modal form of a cantilever beam deflection, although a slight concavity develops toward the plates tip for large Cauchy numbers. To further analyze this process, the empirical flow loading along the plates is estimated by a modified beam theory assuming a distributed load given by a power law. The experimental fitting shows that for large flexibility, the load diminishes at the rear tip. Besides, the progressive deformation of plates is shown to weaken the shedding of vortices and reduce the size of the recirculation bubble. Finally, an affine direct relationship between recirculation bubble aspect ratio and drag coefficient has been proposed in order to quantify the linkage between near wake modifications and hydrodynamic improvement provided by the trailing edge streamlining.

Published under license by AIP Publishing. <https://doi.org/10.1063/5.0046437>

I. INTRODUCTION

The flow around blunt-based bodies represents a widespread situation encountered in many engineering systems, as, for instance, heavy transport, civil structures, and marine applications. These types of flows are characterized by a massive separation at the bluff trailing edges and the subsequent development of a strong wake and a wide recirculating bubble. Such flow separation is responsible for the low base pressure and the vortex shedding. As a result, the blunt bodies have large values of drag and experience important fluctuating forces, which may entail poor aerodynamic performances or structural vibrations.

The previous considerations justify the intense work devoted to develop wake control strategies applied to blunt-based bodies^{1,2} aimed to reduce the fuel consumption, increase the maneuverability of vehicles, or reduce the risk of structural fatigue induced by vibrations. In general, important reductions of the drag resistance by means of base pressure recovery can be achieved using rear systems acting on the body base or the trailing edge. That said, even though

the active systems may increase the performance and optimize the drag reduction, they constitute sometimes difficult solutions to be implemented in practice and demand external energy, what may hinder their suitability in terms of global energy balance.³ Besides, the passive devices present the advantage of its simplicity, although they do not necessarily represent optimal solutions for any flow condition.⁴

Among the passive control strategies for wakes behind blunt-based bodies, the use of base rigid cavities^{5–7} delays the flow detachment and modifies efficiently the base pressure component of the drag. However, such devices do not work optimally for all flow conditions,⁸ what might be partially overcome by using shape optimization techniques to design improved cavities,⁹ or instead, flexible plates that may adapt better to the flow and streamline the trailing edge. In that sense, just a few recent works have studied the effect of implementing flexible parallel plates at the rear of bluff bodies with the main focus on flow-induced vibrations of the plates,^{10–12} showing that a moderate

Part II

Rear cavities of flexibly-hinged rigid plates

Chapter 4

**Numerical analysis of wake
behind a blunt body with rear
hinged cavity.**



Contents lists available at ScienceDirect

Journal of Sound and Vibration

journal homepage: www.elsevier.com/locate/jsv

Flow-induced vibrations of a hinged cavity at the rear of a blunt-based body subject to laminar flow



J.I. Jiménez-González^{a,b,*}, C. García-Baena^{a,b}, J.F. Aceituno^a,
C. Martínez-Bazán^{a,b,c}

^a Departamento de Ingeniería Mecánica y Minera, Universidad de Jaén. Campus de las Lagunillas, Jaén 23071, Spain

^b Andalusian Institute for Earth System Research, Universidad de Jaén, Campus de las Lagunillas, Jaén 23071, Spain

^c Departamento de Mecánica de Estructuras e Ingeniería Hidráulica, Universidad de Granada, Campus Fuentenueva s/n, Granada 18071, Spain

ARTICLE INFO

Article history:

Received 17 September 2020

Revised 1 December 2020

Accepted 4 December 2020

Available online 4 December 2020

Keywords:

Flow-induced vibrations

Bluff body

Passive device

Rear flexible cavity

Multibody dynamics

ABSTRACT

We perform numerical simulations to characterize the flow-induced vibrations (FIV) of a rear cavity with elastically hinged rigid plates, placed as a passive device at the base of a blunt body that is subject to a laminar flow of Reynolds number $Re = 400$. The dynamic response and forcing of plates, wake features and force coefficients are investigated for the range of reduced velocity $U^* = [0, 30]$. Three different regimes of the rotational oscillations are identified. An initial branch of low oscillation amplitude is defined for $U^* < 2.5$, where the plates oscillate in counter-phase (varicose mode) with a frequency f_p that corresponds to the harmonic of the wake vortex shedding frequency $f_p \simeq 2f_w$, and is similar to the natural frequency of the plates, $f_p \simeq f_n$. For intermediate values of U^* , the plates oscillate in phase (sinuous mode) at their natural frequency, with respect to a closer averaged location of plates. Such synchronization regime amplifies the vibration magnitude and defines the upper branch in the amplitude response curve, whose maximum is attained at $U^* = 4.7$. Due to such enhanced vibration, the vortex shedding frequency is now locked-in at the natural frequency of plates, so that $f_p = f_n = f_w$. Finally, for larger values of U^* , a lower branch of moderate amplitude response is defined, which is characterized by the in-phase oscillation of plates, with respect to an more open average position, governed again by the shedding frequency, $f_p = f_w > f_n$. Additionally, a multibody model has been developed to retrieve, from the plates rotational motion, the resultant forces and moments that produce the plates vibration. Such inverse dynamics model is formulated to allow its generalization for configurations of higher dynamical order, and validated against the results obtained from the numerical simulations. The analysis shows that the synchronization regime is mainly promoted by a reduced fluid damping and a forcing moment that acts in phase with the plates motion. The switch in such phase from 0° to 180° occurs after the lock-in, what attenuates the plates response at large U^* . In general, the FIV of plates alters the vortex shedding and near wake pressure, especially during the synchronization regime, inducing an overall increase of the global force coefficients with respect to the static cavity.

* Corresponding author.

E-mail address: jignacio@ujaen.es (J.I. Jiménez-González).

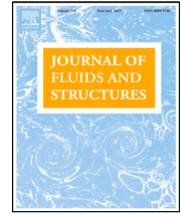
Chapter 5

Drag improvement of a blunt base body using rear flexibly hinged flaps



Contents lists available at ScienceDirect

Journal of Fluids and Structures

journal homepage: www.elsevier.com/locate/jfs

Drag reduction on a blunt body by self-adaption of rear flexibly hinged flaps



C. García-Baena^{a,b}, J.M. Camacho-Sánchez^{a,b}, M. Lorite-Díez^{c,b},
C. Gutiérrez-Montes^{a,b}, J.I. Jiménez-González^{a,b,*}

^a Departamento de Ingeniería Mecánica y Minera, Universidad de Jaén, Campus de las Lagunillas, 23071, Jaén, Spain

^b Andalusian Institute for Earth System Research, Universidades de Granada, Jaén and Córdoba, Spain

^c Departamento de Mecánica de Estructuras e Ingeniería Hidráulica, Universidad de Granada, Campus de Fuentenueva, 18071, Jaén, Spain

ARTICLE INFO

Article history:

Received 24 May 2022

Received in revised form 7 February 2023

Accepted 9 February 2023

Available online 26 February 2023

Keywords:

Drag reduction

Bluff body

Passive control

Flexible flap

Self-adaptive flap

ABSTRACT

We study the aerodynamics of a blunt-based body with rear flexibly-hinged rigid flaps, subject to a turbulent flow of Reynolds number $Re = 12000$, under aligned and cross flow conditions with yaw angle $\beta = 0^\circ$ and $\beta = 4^\circ$. To that aim, different values of the equivalent torsional stiffness are considered, to cover the range of reduced velocity $U^* = (0, 3.48]$ in water tank experiments. The effect of the angular deflection of plates on the drag and near wake flow is analyzed, experimentally and numerically. The results show that, in the range of U^* herein considered, the plates undergo an inwards quasi-static, self-adaptive deflection, which is symmetric for yaw angles $\beta = 0^\circ$ and asymmetric for $\beta = 4^\circ$. In particular, the plates feature small mean deformation angles for values of $U^* < 1$, whereas a sharp and monotonic increase of such deflection occurs for $U^* > 1$, i.e. for lower values of the hinge's stiffness, with an asymptotic trend towards the larger values of U^* . A critical value of reduced velocity of $U^* \simeq 0.96$ is obtained as the instability threshold above which plates depart from their initial equilibrium position. The progressive streamlining of the trailing edge translates into significant reductions of the associated mean drag coefficients. Thus, reductions close to 19% with respect to reference static plates configurations are obtained for the most flexible case of $U^* = 3.48$ for both $\beta = 0^\circ$ and $\beta = 4^\circ$. A close inspection of the near wake reveals that the inwards progressive mean displacement of the plates yields a reduction in the recirculation bubble size. A symmetric evolution of the recirculating bubble is observed for $\beta = 0^\circ$, whereas the bubble becomes asymmetric for $\beta = 4^\circ$, with a larger leeward clockwise vortex. In both cases, the drag coefficient is shown to vary linearly with the global aspect ratio of the recirculating bubble. The analysis of the numerical results shows that the reduced extension of the recirculating bubble significantly alters the formation length and intensity of the eddies size and associated pressure. It is observed that despite the local pressure decrease in the vortices shed from the trailing edges, the plates self adaption reduces their size and prevents the eddies from entering the cavity, thus, creating a dead flow region with a consequent pressure increase at the body base.

© 2023 The Author(s). Published by Elsevier Ltd. This is an open access article under the CC BY-NC-ND license (<http://creativecommons.org/licenses/by-nc-nd/4.0/>).

* Corresponding author at: Departamento de Ingeniería Mecánica y Minera, Universidad de Jaén, Campus de las Lagunillas, 23071, Jaén, Spain.
E-mail address: jignacio@ujaen.es (J.I. Jiménez-González).

Chapter 6

Conclusions and future work

6.1 General conclusions

The work presented in this Thesis focuses on the study and characterization of the near wake and the forces produced on bluff bodies implementing rear flexible plates, used as flow control and aerodynamic drag reduction devices. To that aim, experimental measurements and numerical simulations have been performed to characterize the flow behind the bluff bodies, as well as to identify how these flexible structures affect the aerodynamic forces and their fluctuations, through detailed study of the vortex shedding coherence and flow detachment in the near wake behind the bodies. In particular, this work is focused on the use of base cavities of flexible plates and rigid plates with flexible unions. The study has been conducted for different Reynolds numbers, i.e. considering laminar and turbulent flow regimes, and for different yaw angles. In the following, we summarise the main conclusions and ideas developed and described through Chapters 2-5.

The first Part of the Thesis, which considers cavities of flexible plates, starts with Chapter 2, where we analyze numerically the use of flexible plates, placed at the rear of a blunt-based D-shaped body, as passive control devices in terms of dynamic response and wake forcing, for a laminar Reynolds number of $Re = 500$. Different regimes have been identified in terms of amplitude and frequency responses of the plates, which depend on the values of U^* . First, an initial branch is defined at low values of U^* (high stiffness), which presents a local peak of small displacement response of the plates, that vibrate at the harmonic of the wake shedding frequency $f_p \simeq 2f_{vs}$. This regime is characterized by a varicose mode of vibration, where the plates oscillate in counter-phase. Second, a transition towards a lower branch of weak amplitude response takes place after the local peak of the initial branch, where the plates start to oscillate at the vortex shedding frequency $f_p = f_{vs}$. Subsequently, a lock-in regime develops at intermediate values of U^* , characterized by the synchronization of the vortex shedding and the plates oscillation at its natural frequency $f_p = f_{vs} = f_{1,n}$. The oscillations amplitude is amplified by the synchronization, which define a new upper branch in the amplitude response curve. Differently from the first branch, both the latter lower and upper branches present a sinuous mode of vibration of the plates, that oscillate in phase. Finally, for high values of U^* (low stiffness), the response is characterized by a moderate, modulated amplitude of the oscillations, which display a more irregular dynamics, with multiple frequency components (within the range $5 < f^* < 6.5$), thus, defining a multi-mode regime with no clear phase shift between the plates displacement on account of the continuous change in frequency and amplitude of the time series.

The different dynamic regimes of the plates translate into substantial modifications of the force coefficients. Generally, the weak response of the initial branch

hardly modifies the values of the time-average drag coefficient C_x and the fluctuations magnitude of the lift \hat{C}_y , with the exception of the value of U^* corresponding to the local peak of amplitude, where a slight decrease of 1.7% with respect to the rigid case is reported for the drag, for a plate separation $h_c = 0.8$. It is within the lock-in regime that larger variations of the drag and the lift are observed. In particular, the more intense oscillations of the plates lead to relative growths in C_x of approximately 33% and 44% for $h_c = 0.8$ and $h_c = 0.6$. Interestingly, the lock-in regime induces an attenuation of the lift fluctuations \hat{C}_y of nearly 40%. The latter is partially related to the upstream flow impinging on the outer side of the plates as they move outwards, which induce an inwards lift force component that modulates the peak magnitude. Moreover, for $h_c = 0.6$ a regime is found at the beginning of the upper branch, whereby a low frequency modulation of the plates oscillation amplitude and of the vortex shedding process, translates into simultaneous reduction in the drag and the lift fluctuations amplitudes of 2% and 4.7%, respectively. Besides, the multi-mode regime moderately increases the drag coefficient but considerably affects the lift coefficient, whose fluctuations are amplified due to the more irregular nature of the plates dynamics for low stiffness values.

Finally, a simple quantification of the energy transfer of the plates has been also performed, showing that the lock-in regime represents the best regime to extract energy from the flow. Thus, in view of these results, rear flexible cavities may be considered as valid passive control devices in terms of drag reduction under specific conditions of stiffness and geometry, although the decrease reported for the conditions considered is marginal (approximately 2%). However, the lock-in regime can, in general, be exploited efficiently to reduce the fluctuating nature of forces acting on the body (despite the growth of drag), what is known to attenuate the global structural response of the whole body, e.g. in ocean applications, as risers or slender structures, or to improve the driving stability in transport applications. The latter, together with the important energy transfer from the flow, render such synchronization regime useful for practical applications. Nevertheless, before considering any implementation, a more realistic study, i.e. for turbulent flow and using lower mass ratios, should be undertaken.

In view of the aforementioned results, Chapter 3 presents an experimental study to assess the potential positive effect of the quasi-static reconfiguration of rear parallel plates on the drag coefficient of a slender blunt-based body subject to a turbulent flow with $Re = 12000$, considering lower mass ratios. In general, increasing the flexibility of plates, within the range of Cauchy number $Ca = [0.006, 56.221]$, produces a progressive streamlining of the trailing edge. The latter translates into important reductions of the mean drag coefficient and the amplitude of fluctuations, with maximum reduction values of nearly 14% and 10.5%, respectively. Furthermore, the limit on the potential reduction and the modification of the scaling law between drag force and velocity due to plates reconfiguration, has been analyzed by means of the computation of an equivalent Vogel exponent γ , for which a minimum value of $\gamma = -0.131$ has been found for $Ca = 3.422$.

The analysis of the deformation has revealed that the plates adapt to the flow mainly following shapes corresponding to primary normal modes of a deflected cantilever beam. However, a slight concavity develops towards the tip for large Cauchy numbers, on account of the modifications on the flow loading that the increase of flexibility induces. Such progressive deformation translates into a weakening of the shedding process and a reduction of the recirculation bubble size characterized by an attenuated backflow. From such results, an affine direct relationship between recirculation bubble aspect ratio and drag coefficient has been finally proposed to unveil the

connection between near wake modifications and hydrodynamic improvement provided by the trailing edge streamlining. Such empirical relation might be useful for the design of efficient passive control strategies in engineering systems concerning blunt bodies as e.g. road transport or underwater vehicles.

In Part 2, the use of reduced order systems is considered. In particular, devices consisting of rigid plates with flexible hinges are analyzed. In this way, the problem is simplified, allowing us to deepen in the understanding of the mechanisms responsible for the aerodynamic improvements observed in previous chapters, as well as simplifying the dynamics and implementation of these elements in full-scale vehicles. Therefore, in Chapter 4 we have performed a numerical study of the flow-induced vibrations of a flexibly-hinged cavity, placed at the rear of a blunt-based body, similar to the one in Chapter 3, and subject to a laminar flow of $Re = 400$. The dynamic response of the plates, the wake main features and the force coefficients have been investigated for different values of the hinge stiffness, within the range of reduced velocity $U^* = [1.8, 30]$. Moreover, this fundamental problem has been employed to develop and validate a multibody approach, with the aim to analyze the local flow forcing, and generalize the procedure for configurations of higher geometrical and dynamical complexity.

The results from the numerical simulations reveal the existence of three different flow induced vibrations (FIV) regimes, similar to Chapter 2, in terms of amplitude and frequency responses of the plates. Therefore, at low values of $U^* < 2.5$ (high stiffness), an initial branch is defined, which displays a local peak of small displacement response of the plates, that oscillate in counter-phase and vibrate at the harmonic of the wake shedding frequency $f_p \simeq 2f_w$, similar to the natural frequency of the system and thus $f^* \simeq 1$. After the local peak of the initial branch a transition towards the upper branch of large amplitude response occurs, where the plates oscillate at the vortex shedding frequency $f_p = f_w$. Moreover, a lock-in regime develops at intermediate values of $2.5 < U^* \leq 6.6$, characterized by the synchronization of vortex shedding and the plates oscillation at its natural frequency $f_p = f_w = f_n$ and the amplification of the oscillations of the plates, which present a sinuous (in-phase) mode of vibration. Finally, at high values of $U^* > 6.6$ (low stiffness), a third, lower branch of dynamic response is observed, which features a moderate amplitude of the oscillations. Interestingly, it has been shown that the free rotating case ($U^* \rightarrow \infty$) does not provide with the largest amplitude response, and therefore a moderate value of structural stiffness is necessary to obtain an amplified response (e.g. for energy extraction purposes as seen in Chapter 2). The oscillation of plates modifies the intensity of the vortices and their formation length, although the shedding frequency is however mildly affected by the FIV response. In particular, during the lock-in regime, the shedding is guided by the natural frequency of the plates oscillation, while for the initial and lower branches the frequency is nearly identical to that of the static reference case. These general modifications of the near wake induce growths of the magnitudes of C_x and \hat{C}_y relative to the static case, with the exception of the range of U^* falling in the transition between initial and upper branches. For such small values of U^* , respective highest reductions of 0.5% and 24.95% are attained for the the mean drag coefficient and the amplitude of lift coefficient fluctuations. In particular, it has been shown that the associated FIV mechanisms, characterized by destructive interactions of the different sources of vorticity (i.e. plates motion and vortex shedding due to rear flow detachment), act modifying fundamentally the near wake pressure. Therefore, larger reductions of force coefficients may be expected for larger Reynolds numbers, considered in Chapter 5.

On the other hand, an inverse dynamic multibody model has been developed

to account for the resultant forces and moments that produce the plates rotational motion. Such multibody approach has been satisfactorily validated by means of the comparison against the values of local forces acting on the plates obtained from the numerical simulations. The analysis of the plates excitation has been conducted in terms of the forcing moment and its components, in phase with velocity and the acceleration, which can be used to estimate the fluid damping and inertia, respectively. The study has allowed to infer that the synchronization regime is mainly promoted by a reduced fluid damping and large inertia. In particular, the forcing moment acts in phase with the plates motion within part of the initial branch and the upper branch, what promotes an amplification of the response. However, a phase switch from 0° to 180° has been reported to occur after the lock-in, what causes an attenuation of the plates oscillations at large U^* . Although a multibody model cannot reproduce the fluid-structure interaction and the stress distribution through the plates surfaces, the accurate estimation of the resultant forces and moments results without incurring in a high computational cost is a clear advantage of its application. Such feature makes this methodology also particularly suitable for experimental tests, where the local forcing is not always directly registered but it is easy to measure the structure displacements, e.g. by means of visualizations techniques as the ones used in Chapter 4.

Similar to Chapter 3, Chapter 5 considers the study of the aerodynamics of a D-shaped blunt body that implements rear flexibly-hinged rigid flaps and is subject to a turbulent flow, at $Re = 12000$, for different yaw angles, namely $\beta = 0^\circ$ and $\beta = 4^\circ$. To that aim, different flap-embedded plate properties are considered, which yield associated reduced velocities in the range $U^* = [0.01, 3.484]$. In particular, the effect of the system on the drag, plates displacement and near wake flow is analyzed, by means of experiments and complementary numerical simulations.

The results show that, in the range of U^* considered, the plates undergo an inwards quasi-static reconfiguration, which is symmetric for yaw angles $\beta = 0^\circ$ and asymmetric for $\beta = 4^\circ$. In that regard, low mean deformation angles Θ are observed for values of $U^* < 1$, whereas a sharp and monotonic increase of Θ occurs for $U^* > 1$, i.e. for lower values of the hinge stiffness, with an asymptotic trend towards the larger values of U^* . Consequently, a progressive streamlining of the trailing edge is induced for both values of the incident yaw angle β . The latter translates into significant reductions of the associated mean drag coefficients, specially for $U^* > 1$, with maximum values equal to 18% and 19%, obtained for the most flexible case $U^* = 3.484$, for $\beta = 0^\circ$ and $\beta = 4^\circ$, respectively. In computing the evolution of the Vogel exponent γ to evaluate the effect of the rear configuration on the recirculation bubble aspect ratio, it has been observed that $\gamma \simeq 0$ for low Ca number ($U^* < 1$) but displays negative values for $Ca > 3.423$ ($U^* > 1.154$).

A close inspection of the near wake reveals that the inwards progressive mean displacement of the plates yields a reduction in the recirculation bubble size. The aforementioned stems from an increase of the flow momentum towards the axis in the y coordinate, which results in a narrowing of the traverse bubble height and shortening of the bubble length. A symmetric evolution of the recirculating bubble is observed for $\beta = 0^\circ$, whereas the bubble becomes asymmetric for $\beta = 4^\circ$, with a larger leeward clockwise vortex. The reduced extension of the recirculating bubble significantly alters the formation length and intensity of the eddies pressure. In particular, it is observed that despite the local pressure decrease in the vortexes shed from the trailing edges, the plates reconfiguration prevents the eddies from entering the cavity, thus, creating a dead flow region with a consequent pressure increase at the body base.

In summary, the work presented in Part 2 shows that a simple system of flexibly-hinged rigid plates with a low number of degrees of freedom is able to induce significant drag reductions based on trail reconfiguration. Therefore, this might constitute an effective alternative to be used as a drag reducer in bluff vehicles, without the complex dynamics and associated disturbances observed in purely flexible foils.

6.2 Future work

Along this Thesis some questions have been left open to be addressed in the future, in order to gain a more comprehensive understanding of the problems considered and the results described throughout this dissertation. In this sense, the use of fluid-structure interaction software, such as OpenFOAM, has proven to be useful in the prediction of the wake behaviour and forces on the body with different flexible and flexibly-hinged devices. Consideration of more realistic bodies and higher Reynolds numbers employing more accurate turbulence models, like URANS or LES, could be a natural course of future works. Thus, the extension of the present studies to consider 3D models of heavy-duty vehicles should be targeted, such as those similar to the Ahmed body. In particular, different investigations focused on the study of these types of models are currently being experimentally and numerically conducted by members of the group, considering not only the use of rear flexible cavities but other drag reduction strategies such as base blowing. The studies in Chapter 2 should be extended to consider lower mass ratios, which present an increase of the dynamic response and yield larger drag reductions and fluctuations amplitudes. In particular, preliminary analysis of the peak of the initial branch for lower mass ratios than the ones used in Chapter 2 show drag reductions that are twice those in the original study. On the other hand, the flexibly-hinged cavity simulations for few degrees of freedom have proven to be a really quick and precise first approximation to the real problem, as seen in Chapter 5. Therefore, the design of real drag reduction devices for 3D vehicles would benefit from the performance of numerical studies conducted using this kind of approach.

The numerical and experimental results obtained in the present dissertation on the use of rear cavities of flexible plates or rigid plates with flexible joints to improve the aerodynamic performance and extend their use to a wide range of flow conditions on bluff bodies are promising. However, the results are circumscribed to well controlled, reduced-scale laboratory tests or numerical simulations, with maximum Reynolds numbers of order 10^5 . Moreover, the suitability of the proposed structures has been satisfactorily proven in terms of drag reduction and wake control in simplified blunt-based bodies. Thus, the design of real or improvement of actual rear devices for heavy-duty transport vehicles would require further investigation. In that regard, they should be widely tested in real vehicles and under more realistic conditions. For all of the above, experimental results should be extended in wind tunnel tests considering larger Reynolds numbers and more complex models, where measurements of aerodynamic forces, deflection of the plates and base pressure would be carried out. On that matter, experiments are currently being conducted in a larger facility, using real-truck models, for $Re \sim 10^6$. Moreover, some of these structures have been preliminary constructed, implemented in full-scale vans provided by our industrial partner in this line of research, and tested in a circuit, with promising results. Thus, a new set of experiments will be designed, for which the devices showing better performance will be constructed and implemented in real trucks. Measurements of the base pressure recovery, together with fuel consumption saving on a real case scenario

will be obtained as a results of these tests, which will corroborate the outcomes of the present Thesis. To that aim, proper selection of the device and material properties are paramount. In this regard, flexibly-hinged cavities of rigid plates have proven to be a simpler approximation to passive reconfiguration. Thus, these kinds of devices will be first assessed. This selection will be then accompanied by the design of a functional truck anchoring system and an industrial production planning, with the aim to develop fully operational retractable or folding devices ready to be used.

Finally, thanks to the research stay of the candidate at the Sorbonne Université de Paris (France), an investigation on the dynamics of bio-inspired solutions will be open. In particular, the studies initiated on the beating mechanics of Diptera will be continued. Some preliminary results of this work are included in Appendix A. Future works will include the performance of additional experiments considering different types of wings and veins disposition. The latter will be complemented with numerical simulations, which will use the deformations obtained in the experiments as input. The use of stereo-PIV to characterize the flow and vortex shedding of this interesting bio-inspired problem is also considered. It is expected that a better understanding of this problem could help in the design of new flexible devices, since thanks to the relatively simplicity of the insect flight mechanics and millions of year of natural evolution could inspire us in proposing new engineering applications in the aerodynamics improvement field.

Appendix A

Forces and 3D deflection study of insect-inspired two-vein flapping wings

This Appendix is comprised, in part, in the paper: "Insect-inspired two-vein flapping wings with anisotropic rigidity", by C. García-Baena, R. Godoy-Diana, R. Antier, J.I. Jiménez-González, C. Gutiérrez-Montes & B. Thiria, under preparation (2022).

A.1 Introduction

Fluid-structure interaction phenomena and the use of flexible devices are common in nature. Examples are plants, fishes and flying vertebrates, like birds and bats. For instance, the role of flexibility is major for the efficient locomotion of animal, being it an essential ability for the survival of animal species. It allows animals and organisms to move, feed, reproduce or escape from an attack. The differences in the medium and environment have led species to develop a multitude of means of locomotion [85]. In the case of flight or swimming, the surrounding fluid is set in motion by the animal, propulsion transfers momentum to the fluid which is accelerated and pushed into the wake behind the animal. To generate this propulsion, nature has developed two methods. The first method, is the one used in particular by jellyfish or squid, which consists of the contraction of a rear flexible cavity at the back of the animal (for example, the bell in jellyfish) that allows the fluid to be expelled and the animal to be pushed forward at the same time [86]. The second method, is based on the oscillating movement of a part of the body or the body as a whole. It brings together a wide variety of strategies ranging from the undulation of the body, as for anguilliformes, to the flapping of the wings for birds, bats or insects, through the flapping of the tail for fish.

Beaten flight is based on two fundamental elements: a wing and a flapping motion. The wing makes it possible to oppose a large surface to a flow of fluid, and the flapping movement induces a relative speed between the wing and the air. Insects beaten flight is really interesting for engineering and maintains a close relationship with flexible passive aerodynamic drag reduction strategies because of its flight mechanics. In that regard, insects have no muscles in their wings unlike birds or bats. Instead, the beats of insects are driven by two antagonistic groups of power muscles placed at its thorax and the force is funneled to the wing via a complex hinge mechanism [87] to control the wing pitch during flight. It has been demonstrated that aerodynamic and wing inertia forces driven by the anisotropic flexibility of the wing are sufficient to pitch the wing passively without the aid of any extra muscles [88].

In the air or in the water, the propulsion uses the viscosity of the fluid and its inertia. The propulsion mechanisms are different according to the characteristics of the flow and according to the size of the animal. To estimate the relative influence of viscous forces and inertial forces in the relative displacement of an object with respect to the surrounding flow, Reynolds defines the dimensionless number,

$$Re = \frac{\rho_f u_\infty h}{\mu_f} \quad (\text{A.1})$$

where u_∞ is the flow velocity, h the model characteristic size (length of a fish, or wingspan of an insect for example), ρ_f the density of the fluid and μ_f is the fluid dynamic viscosity. To move, the organism relies on the fluid which resists thanks to its viscosity. When $Re \gg 1$, for very large objects such as airplanes, the viscous effects are confined to the boundary layers near the surface, and inertia dominates in front of the viscous effects outside the boundary layer. The acceleration of the fluid around the object is the origin of the displacement, the acceleration of the air induces a pressure gradient around the object, which results in the creation of the aerodynamic forces. When $Re \sim 1$, at an intermediate Reynolds number, for species with a size order of $O(10^{-2} - 10^{-3})$ m, the propulsion comes from a competition between the viscous effects and the inertial effects. The Reynolds number of insects ranges from $O(10^1 - 10^4)$ [89], this wide range is due to the great diversity of sizes of flying insects.

Insects are the only species, with the Hummingbird, to be able to hover, that means to be able to maintain a fix position in the air, a greatly demanded ability for modern drones and other unmanned vehicles. For all species, a determined cruising speed is needed, propulsion performance at cruising speed depends on the dynamics of the flow behind the wing. At the end of each flapping motion, vortices are released into the wake behind the wing. The behavior of the vortex street is resultant from the way in which the vorticity and pressure evolve into the wake. The kinematics of the wing is the key element controlling the release of the vortices. To characterize the propulsion, we use the Strouhal number,

$$St = \frac{fA}{u_\infty} \quad (\text{A.2})$$

Where f is the flapping wing frequency, A is the flapping amplitude and u_∞ is the advance velocity of the animal. Triantafyllou et al. [90] and then Taylor [91] showed that there is a range of Strouhal numbers favored by animals. For a St varying from 0.2 to 0.4, the configuration of the wake is optimal for propulsion, and maximum efficiency is observed, making the range of Strouhal numbers seen in nature very narrow while the range of sizes of all the existing species is wide and really diverse.

The concentration of the Strouhal number in this narrow range is explained by the configuration of the wake behind the oscillating wing (or fin). Vandenberghe et al. [92] showed with a rigid wing that the oscillation frequency had to exceed a limit value to generate a spontaneous advance movement. For frequencies above the limit frequency, the feed rate increases linearly with frequency. For frequencies below this limit, the flow around the wing is symmetric. For frequencies above this limit, the symmetry of the flow is broken and the wake takes the form of an inverted von Kármán street. The breaking of the symmetry of the wake is the origin of the propulsion. When the beat frequency is too high, Godoy-Diana et al. [93] showed that the jet behind the wing is deflected and the deviation of the jet comes from the asymmetry of the inverted vortex street.

The remarkable performance of insects flight has prompted engineering to take inspiration from nature. Artificial flying systems are increasingly using mechanisms discovered in insects [94]. With this in mind, biomimicry is a booming field in taking advantage of the solutions proposed by evolution to respond to certain problems. Insect wings are composed of a membrane, made of epidermal cells, and a network of veins, or ribs, supplying the wing with oxygen and nutrients [95]. Observing the network of veins more closely, we see that the veins are located in the creva of folds. These corrugations of the wings have two effects. First, the ribs give the wing a streamlined shape, and inside the folds of the ribs we witness the creation of vortices. The inside vorticity reinforces the streamlined shape of the section and affects the pressure distribution. The vorticity created inside the folds also decreases the friction of the fluid on the wing. Another advantage concerning the use of folds in insect wings is proposed by Wootton [96], namely the relief of the wing, due to the ribs, which affects its bending and torsion stiffness. In particular, the presence of folds induces a curvature asymmetry of the wing depending on whether flexion is either ventral or dorsal. The folds point towards the back of the insects and this specificity has the effect of limiting the dorsal flexion of the wing. On the other hand, the ventral flexion is amplified because of the buckling of the structure which flattens the folds. The multitude of orientations of the ribs generates an asymmetry of deformation of the wing in several directions making the wing bending asymmetry to produce an increase in aerodynamic forces compared to the symmetrically bending case [96].

It is not known yet if insects have evolved to save energy by optimizing flapping performance. However, several studies show that the flexibility at the wings, provides with an optimization of the performance for a system of artificial flapping flight [97], [98]. During flapping, the wings passively deform to increase beating efficiency. Passive deformation allows to benefit from the elastic deformation energy of the wings by absorbing or releasing energy to the fluid. Using an artificial insect equipped with flexible wings, Thiria and Godoy-Diana [99] showed the benefit of flexibility along the chord in the performance of an artificial insect. Flexibility leads to a greater beat amplitude for the same energy being provided when the wing oscillates at a frequency close to its resonant frequency f_n . Therefore, flexibility modulates the phase shift between the leading edge and the trailing edge by controlling the wing curvature dynamics. The control of the temporal evolution of the shape of the wing optimizes the aerodynamics of the insect. Furthermore, using PIV measurements (Particle Image Velocimetry), Mountcastle and Daniel [100] showed that the flexibility of the wing amplified the flow generated and redirected it in a direction more favorable to the insect. The relatively simplicity of the insect flight mechanics and millions of year of natural evolution, could inspire the creation of new engineering applications in the aerodynamics improvement field.

A.2 Problem description

The work discussed here is an ongoing investigation in line with previous studies developed by R. Antier [101] on the analysis of the aerodynamics of a flapping insect-inspired flexible wing and the reinforcement of a flexible membrane by a network of heterogeneous veins to generate the maximum propulsion with a wing beat. Flapping flight is described as a rotational movement of the wings around an axis, where the leading edge of the wing is the one in front when the insect moves forward and the trailing edge is the one at the rear for the same case. The transition from downstroke to upstroke is called supination, and the transition from upstroke to downstroke

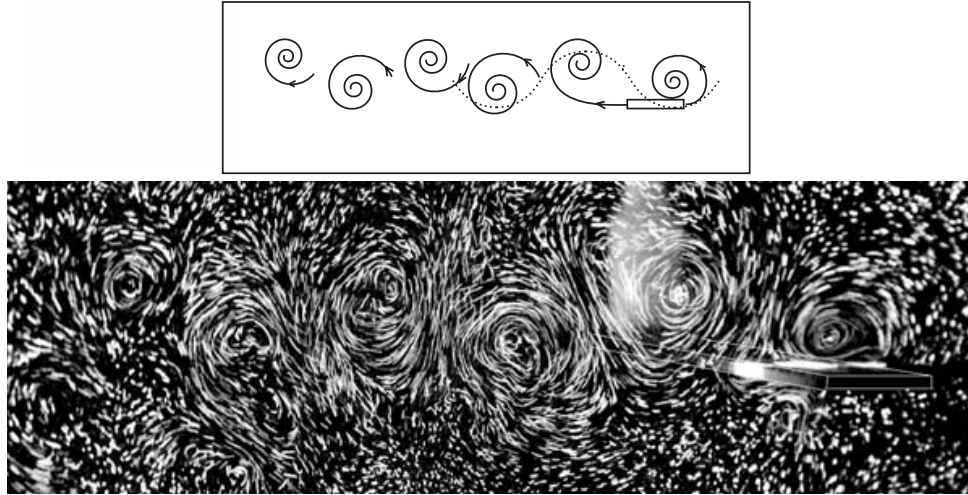


Figure A.1: The wake behind a rotating wing at low Reynolds number (≈ 500) exhibiting an 'inverted' von Kármán vortex street [92]

is called pronation. During these transitions, it has been observed that the wings reorient themselves very quickly, giving rise to mechanisms of unsteady aerodynamics [102], [103]. The combination of these different parameters produces a beat trajectory approaching the description of a lemniscate [104], [105].

Two vortices are released into the wake per beat cycle. These vortices are formed due to the direction change in the movement of the wing, and grow during beating thanks to the passage of fluid from the boundary layer to the vortex being formed. When the wing rotates, a highly structured wake is formed, Fig. A.1. With each flapping period, two counter-rotating eddies are shed into the wake. An 'inverted' von Kármán vortex street is clearly observed producing a flow pattern characteristic of thrust production [92].

When the direction of flapping changes, a vortex is released into the wake at the rear of the wing, called the trailing edge vortex (TEV) and, in the same manner, during supination and pronation a vortex is also formed at the leading edge. This leading edge vortex (LEV) rotates in the opposite direction with respect to the TEV and during the beat, the LEV grows and moves towards the trailing edge, where is destroyed or absorbed by the next TEV produced by the change in beat direction.

During flapping, the wings passively deform to increase flapping efficiency. Passive deformation makes possible to take advantage of the elastic deformation energy of the wings by absorbing or releasing energy to the fluid [98]. Flexibility leads to a greater flapping amplitude for the same energy supplied than a rigid one when the wing oscillates at a frequency close to its resonant frequency. Then, flexibility modulates the phase difference between the leading edge and the trailing edge by controlling the curvature dynamics of the wing. The control of the temporal evolution of the shape of the wing makes it possible to optimize the aerodynamics of the insect, redirecting it in a direction more favorable to the insect [106]. One of the advantages of flexible wings is to replace the rotational movements of the wing by a passive deformation, no longer needing to supply energy to turn its wings during supination and during pronation.

Quasi-stationary mechanisms produce an asymmetric pressure field around the wing, being the aerodynamic force the resultant of the pressure field normal to the wing. For a rigid plane wing, the direction of the resultant pressure forces is directly perpendicular to the wing. For a flexible wing, the direction depends on the curvature

since the local pressure forces are redirected. Propulsion force is the average force in the direction of advance and is the sum of the local forward aerodynamic forces. An efficient flight is that where the propulsion is larger than aerodynamic drag. At the same time, the curvature decreases drag by reducing the projected area perpendicular to the incident flow, and also reduces the effective angle of attack and delays boundary layer detachment. However, the curvature must not exceed a certain value or it will become too great, decreasing flight performance because of the fluid premature detachment [98]. During pronation or supination, the curvature of the wing generated by the rotation has the effect of delaying the displacement of the trailing edge relative to the leading edge, keeping the leading edge eddy attached to the wing and rapidly evacuating the trailing edge vortex [107] when reversing the curvature, in supination or pronation.

Flexibility bends the wing under inertial forces and the inertia imposes the amplitude of flexion of the wing. The damping of the air generates a delay of the trailing edge with respect to the leading edge but if the trailing edge is in phase with the leading edge, the wing will be flat at the instant of maximum speed in the middle of the beat and no propulsive force will be created. If the trailing edge is too out of phase with respect to the leading edge, the same phenomenon is encountered. Flexibility is most useful when the wing is bent at the instant when its speed is maximum and the trailing edge must lag behind the leading edge [98].

Wing mechanics are based on a limited number of veins, each with their own direction. The network of veins is heterogeneous and confers an anisotropic behavior to the wing in many different species [108]. It has been observed that the two most important veins, or two sets of veins (Fig. A.2a,b), are found on the leading edge and in a diagonal direction of the wing (radial vein). Maintaining a sufficiently large stiffness in the leading edge is essential to allow the wing to cut through the air when flapping [109]. The diagonal direction is also observed to be stiffened by the network but its role is less obvious. Several studies show a flex of the wing around this rigid axis [95], [110]–[112], but no conclusion has yet been issued as to its usefulness in the production of aerodynamic forces. This work try to provide responses to previous issues regarding the role of directional stiffness in forces exerted by flapping flexible wings. To that aim, an experimental study is performed, whose details are subsequently given.

A.3 Experimental set-up

This present study is focused on an artificial model of flapping flight inspired by the wings of Diptera, enlarged to ease the force and displacement measurements, as in the work of R. Antier [101]. The wings consist of a membrane made of a film of polyethylene terephthalate (PET), of 30 μm thickness and a Young's modulus of 4 GPa. The flexible membrane is supported with two 3D printed polylactic acid (PLA) veins with a Young's modulus of 4 ± 0.3 GPa. One of the veins is located at the leading edge, while the second one is placed on the wing membrane forming an angle β with the leading edge. The veins are glued to each side of the membrane using Teroson SB2444 rubber glue, an elastic adhesive that allows significant sliding of the membrane between the veins without separation. The veins are 1 mm wide, being the thickness at each side of the wing equal to 480 μm and 240 μm for the vein at the leading edge and the radial vein, respectively. The angles β tested for the present work are $\beta = [10, 15, 20, 40]^\circ$. The leading edge vein is extended 3.5 mm towards the center of the ellipse in order to connect the wing to the beating mechanism. The

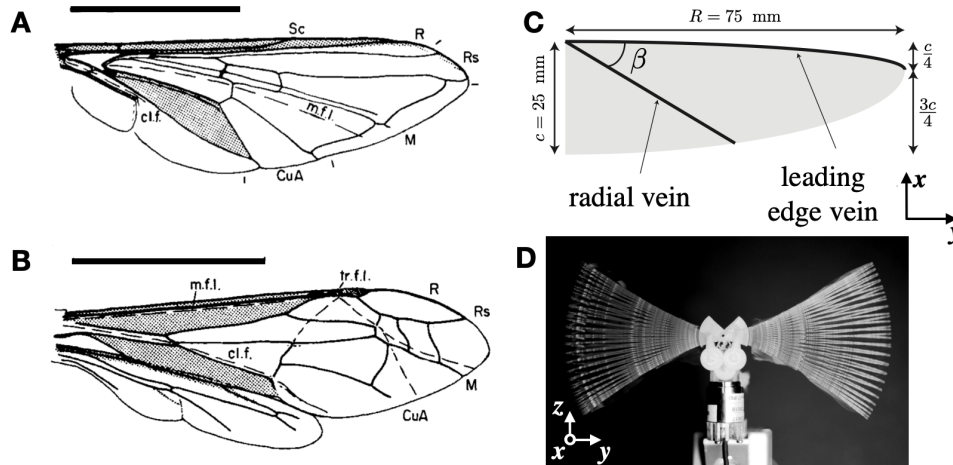


Figure A.2: (a) and (b) are two examples of different rigidity distribution in insect wings depending on the species [110]. Supporting areas (stippled), deformable areas (unstippled) and flexion lines (dashed) in (a) *Syrphus ribesii* (Diptera) and (b) *Vespu lu germanicu* (Hymenoptera). median flexion line (m.f.l.), claval furrow (cl.f.) and transverse flexion line (tr.f.l.). Scale lines = 5 mm. (c) Model wing used in the present work. (d) Frontal view of the system mounted on the force sensor with several snapshots superposed to illustrate the flapping wing motion. [115]

model has been implemented with a Zimmerman planform wing, which is inspired by a simplified hummingbird wing shape [113] (see Fig. A.2c). However, very similar forms are found in multiple kinds of insects [107], [111], [112], [114].

The mechanism used to simulate the wing motion (Fig. A.2d) is the system designed by the University of Delft [116], which produces a plane sinusoidal beat with an amplitude of 32° and frequencies ranging from 5 to 30 Hz. The beat is not symmetrical, with a median angle of 8° below the horizontal plane. The wings were fitted into the arms of the flapping system and fixed using glue.

In the experiments, the deformation of the wings were measured using three high speed cameras working at 1000 fps (a Phantom M120 and two Phantom M320S), which were placed around the model in different locations and angles, as seen in Fig. A.3(a), to register simultaneously all the points printed on the wings for tracking purposes (Fig. A.3b, c). A 3D calibration and synchronization of the camera system was conducted previous to each test. From the recordings, a 3D tracking and point reconstruction of the printed wing by digital image correlation was performed. Further details on the 3D reconstruction of the points in the wings, the system calibration and the software used can be found in [117].

The aerodynamic forces induced by the flapping of the wing were measured using a 6-axis load cell (Schunk FT-Nano 17), with force resolution of 0.0015 N and acquisition frequency of 10000 Hz. The flapping system was attached to the force sensor with plastic parts to avoid spurious currents. The three cameras and the force sensor were synchronized and triggered externally using a National Instruments NI-9205 acquisition card.

A.4 Results

A set of experiments were carried out to measure the force of propulsion as a function of the angle between the veins β for a range of frequencies corresponding to that of Diptera (Fig. A.4). Simultaneously, we measured the time deformation of the wings during the beating cycle (Fig. A.5). Experiments show that the mean propulsion force

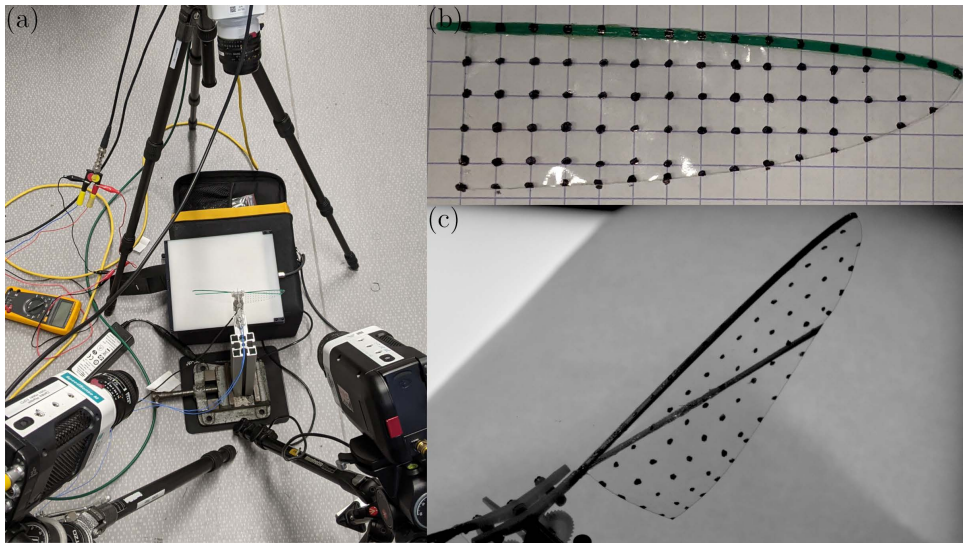


Figure A.3: Set-up of the experiment (a), with the prototype of the printed Zimmerman wing without radial vein (b) and the view from one of the cameras for a 20° radial vein.

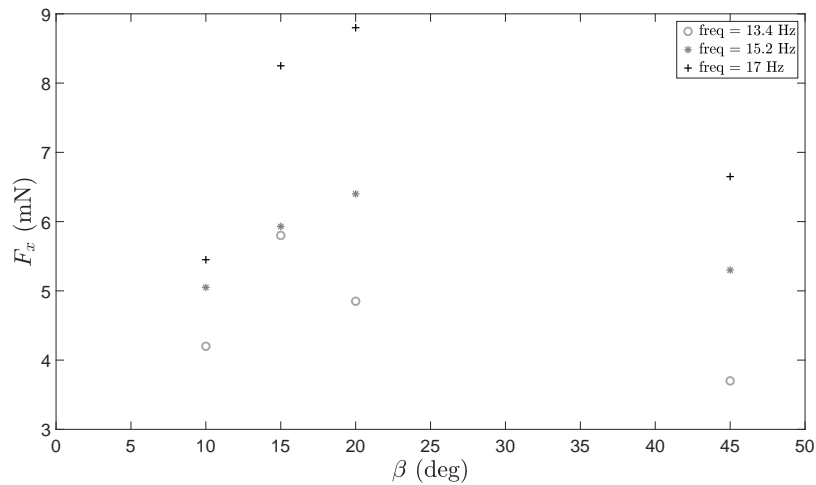


Figure A.4: Mean force in the advance direction of the model for different angles of the radial vein β and beating frequencies.

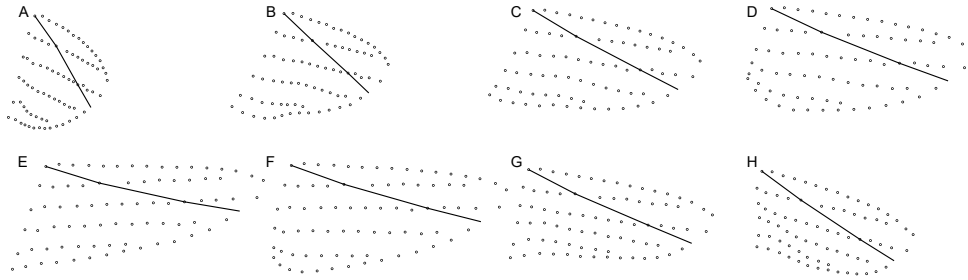


Figure A.5: Beating cycle for a wing with a $\beta = 10^\circ$ and beating frequency of 13.4 Hz.

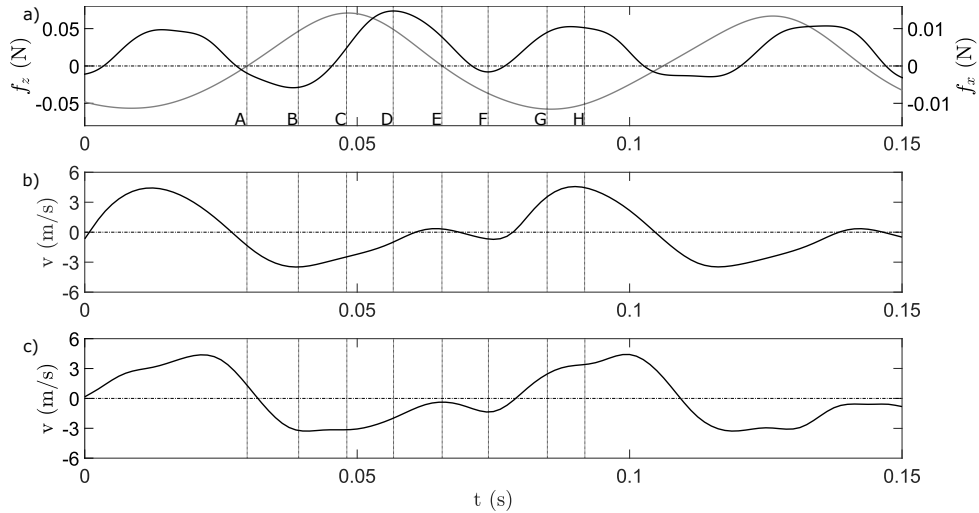


Figure A.6: Forces in the advance (black) and vertical direction (grey) of the model with each corresponding instantaneous wing deformation a), mean velocity of the leading edge points b) and mean velocity of the trailing edge points c).

F_x is maximum for an angle between the veins β in the range of 15 to 20 degrees as reported by [101], being the optimal beating frequency for veins with an angle of $\beta = 15^\circ$ equal to 13.4 Hz, and for $\beta = 20^\circ$ equal to 17 Hz, as shown in Fig. A.4. It is observed that the propulsive force increases as the beat frequency also increases inside the range from 10 to 20 Hz. The measurements show that the maximum force is reached when the coupling between the projected surface and the angle of deflection of the wing is optimal. In particular, although not shown, it is seen that the forces were largest for the configurations presenting the greatest projected areas of the wing in the perpendicular plane to the forward direction. In particular, the maximum value of the force was measured when the maximum angle of deflection of the wing was as close as possible to the angle of incidence of the wind.

Figs. A.5 and A.6 show the wing 3D deformation and the temporal evolution of the forces in the horizontal and vertical direction with the temporal mean velocity of the leading and trailing edge for the case with $\beta = 10^\circ$ and a beating frequency of 13.4 Hz, for two beating cycles. The cycle starts at A, where the wing is at the bottom position moving up at low velocity, whereas a phase shift between the LE and TE occurs due to the inertial forces and flexibility, which is a constant for all the cycle. At B the wing moves up, reaching the maximum upward velocity for the LE and TE, increasing the drag and lift. The maximum lift force is reached at C, where the velocity of the LE is decreasing but the TE has kept it at its maximum, being the inertia of the free surface of the wing below the second vein which produces the majority of the lift force. An increase of thrust can be also observed, due to the

changing curvature of the wing, which is increasing the surface in the perpendicular plane to the forward direction. Then, in D the lift starts to decrease, the TE peak pointing downward can be observed at the end phase of the wing beat, and one of the maximum values of thrust is reached stemming from the force produced by the inertia of the wing free surface. Subsequently, the wing almost stops at the top position E, generating a null lift and small values of thrust associated to the wing remaining upward inertia. As the wing moves downwards in F, a change in curvature occurs in the opposite direction, increasing the drag and inducing negative values of lift. When the wing reaches the minimum value of lift at G, the wing shape has changed completely to increase thrust. The curvature is maximum at H, keeping a high value of thrust while reducing the negative value of the lift produced by the wing inertia. As can be seen in Fig. A.6, both lift and thrust mean values are positive. The phase shift between the LE and TE velocities produced by the flexibility of the wing is notorious in all the beating cycles, producing the thrust force and the lemniscate movement of the wing (Fig. A.5), with only an up and down linear movement.

A.5 Conclusions and future work

An artificial model of flapping flight inspired by the wings of Diptera implementing two veing has been constructed. Aerodynamic forces and wings deformations have been simultaneously measured to characterize the performance of the beating mechanism for different configurations of the veins and flapping frequencies. Measurements show that propulsive forces are largest for veins angles in the range between 15 and 20 degrees. The latter is in agreement with values of angles in real Diptera wings, where the two main veins are form an angle β close to 15 degrees with respect to each other. The good correlation between the optimum angle, in terms of propulsion, determined with our model wings and the angle observed on the wings of Diptera suggests that the wings of Diptera have evolved to this bi-reinforced configuration for aerodynamic reasons. To strengthen a membrane with the aim to achieve an effective flapping wing, the pleats must be positioned on the leading edge and in a direction oriented close to 15 to 20 degrees with respect to the leading edge, the angle varying as a function of the beating frequency.

The experimental results agree with the previous work of [101] and provides detailed information on the time evolution of the passive flexible reconfiguration observed in insects flight. In the following, all the data gathered in the tests will be thoroughly analysed for all the different veins angles and beating frequencies considered in the experiments. In particular, focus will be placed on the cases with largest values of thrust force. It is expected that the comprehensive data recorded will help to understand the underlying mechanisms and to improve flight performance. Complementary numerical simulations are proposed to delve into the subject and the physics behind it in future investigations. All of the above is expected to provide with a good opportunity to extrapolate some of the results obtained or concepts learned to real life engineering applications.

Bibliography

- [1] International Energy Agency, “Emissions from fuel combustion,” 2018.
- [2] International Energy Agency, “Tracking transport,” 2019.
- [3] Y. Qu, T. Bektaş, and J. Bennell, “Sustainability SI: Multimode multicommodity network design model for intermodal freight transportation with transfer and emission costs,” *Networks and Spatial Economics*, vol. 16, 2016.
- [4] W. Hucho *et al.*, *Aerodynamics of Road Vehicles, 4th Edn.* SAE International, 1998.
- [5] W. Hucho and G. Sovran, “Aerodynamics of road vehicles,” *Annual Review of Fluid Mechanics*, vol. 25, no. 1, pp. 485–537, 1993.
- [6] Work of the US Gov. Public Use Permitted, *Spinoff 2008: 50 years of NASA-Derived Technologies (1958-2008)*, 2008.
- [7] L. Ruiying, “Aerodynamic drag reduction of a square-back car model using linear genetic programming and physic-based control,” Ph.D. dissertation, 2017.
- [8] M. Grandemange, “Analysis and control of three-dimensional turbulent wakes: From axisymmetric bodies to road vehicles,” Ph.D. dissertation, ENSTA, Paris-Tech, 2013, ISBN: 9789085783442.
- [9] H. Choi, J. Lee, and H. Park, “Aerodynamics of heavy vehicles,” *Annual Review of Fluid Mechanics*, vol. 46, no. 1, pp. 441–468, 2014.
- [10] J. Peng, T. Wang, T. Yang, X. Sun, and G. Li, “Research on the aerodynamic characteristics of tractor-trailers with a parametric cab design,” *Applied Sciences (Switzerland)*, vol. 8, 5 2018.
- [11] R. M. Wood, “A discussion of a heavy truck advanced aerodynamic trailer system,” *SOLUS-Solutions and Technologies LLC*, 2006.
- [12] E. Sanmiguel-Rojas, A. Sevilla, C. Martínez-Bazán, and J. M. Chomaz, “Global mode analysis of axisymmetric bluff-body wakes: Stabilization by base bleed,” *Physics of Fluids (1994-present)*, vol. 21, no. 11, p. 114 102, 2009.
- [13] J. O. Pralits, L. Brandt, and F. Giannetti, “Instability and sensitivity of the flow around a rotating circular cylinder,” *Journal of Fluid Mechanics*, vol. 650, 513–536, 2010.
- [14] A. Sevilla and C. Martínez-Bazán, “Vortex shedding in high Reynolds number axisymmetric bluff-body wakes: Local linear instability and global bleed control,” *Physics of Fluids (1994-present)*, vol. 16, no. 9, pp. 3460–3469, 2004.
- [15] V. Parezanović and O. Cadot, “Experimental sensitivity analysis of the global properties of a two-dimensional turbulent wake,” *Journal of Fluid Mechanics*, vol. 693, pp. 115–149, 2012.
- [16] G. Vilaplana, M. Grandemange, M. Gohlke, and O. Cadot, “Global mode of a sphere turbulent wake controlled by a small sphere,” *Journal of Fluids and Structures*, vol. 41, 2013.

- [17] B. Khalighi, S. Zhang, C. Koromilas, *et al.*, “Experimental and computational study of unsteady wake flow behind a bluff body with a drag reduction device,” SAE Technical Paper, Tech. Rep., 2001.
- [18] E. Sanmiguel-Rojas, J. I. Jiménez-González, P. Bohorquez, G. Pawlak, and C. Martínez-Bazán, “Effect of base cavities on the stability of the wake behind slender blunt-based axisymmetric bodies,” *Physics of Fluids (1994-present)*, vol. 23, no. 11, p. 114 103, 2011.
- [19] A. Evrard, O. Cadot, V. Herbert, D. Ricot, R. Vigneron, and J. Détery, “Fluid force and symmetry breaking modes of a 3d bluff body with a base cavity,” *Journal of Fluids and Structures*, vol. 61, pp. 99 –114, 2016.
- [20] M. Lorite-Díez, J. I. Jiménez-González, C. Gutiérrez-Montes, and C. Martínez-Bazán, “Drag reduction of slender blunt-based bodies using optimized rear cavities,” *Journal of Fluids and Structures*, vol. 74, pp. 158 –177, 2017.
- [21] M. Lorite-Díez, J. I. Jiménez-González, L. Pastur, C. Martínez-Bazán, and O. Cadot, “Experimental analysis of the effect of local base blowing on three-dimensional wake modes,” vol. 883, A53, 2020.
- [22] M. Grandemange, D. Ricot, C. Vartanian, T. Ruiz, and O. Cadot, “Characterisation of the flow past real road vehicles with blunt afterbodies,” *International Journal of Aerodynamics*, vol. 4, 1/2 2014.
- [23] M. Grandemange, O. Cadot, A. Courbois, *et al.*, “A study of wake effects on the drag of Ahmed’s squareback model at the industrial scale,” *Journal of Wind Engineering and Industrial Aerodynamics*, vol. 145, 2015.
- [24] G. Bonnavion, O. Cadot, A. Évrard, *et al.*, “On multistabilities of real car’s wake,” *Journal of Wind Engineering and Industrial Aerodynamics*, vol. 164, 2017.
- [25] S. R. Ahmed, G. Ramm, and G. Faitin, “Some salient features of the time-averaged ground vehicle wake,” Society of Automotive Engineers, Inc. Warrendale, PA, Tech. Rep., 1984.
- [26] L. Henning, M. Pastoor, R. King, B. R. Noack, and G. Tadmor, “Feedback control applied to the bluff body wake,” in *Active flow control*, Springer, 2007, pp. 369–390.
- [27] M. Lorite-Díez, J. I. Jiménez-González, C. Gutiérrez-Montes, and C. Martínez-Bazán, “Effects of rear cavities on the wake behind an accelerating D-shaped bluff body,” *Physics of Fluids*, vol. 30, no. 4, p. 044 103, 2018.
- [28] M. Pastoor, L. Henning, B. R. Noack, R. King, and G. Tadmor, “Feedback shear layer control for bluff body drag reduction,” *Journal of Fluid Mechanics*, vol. 608, pp. 161–196, 2008.
- [29] S. Krajnović and J. Fernandes, “Numerical simulation of the flow around a simplified vehicle model with active flow control,” *International Journal of Heat and Fluid Flow*, vol. 32, no. 1, pp. 192–200, 2011.
- [30] R. Verzicco, M. Fatica, G. Iaccarino, P. Moin, and B. Khalighi, “Large eddy simulation of a road vehicle with drag-reduction devices,” *AIAA Journal*, vol. 40, no. 12, pp. 2447–2455, 2002.
- [31] H. Choi, W. P. Jeon, and J. Kim, “Control of flow over a bluff body,” *Annual Review of Fluid Mechanics*, vol. 40, no. 1, pp. 113–139, 2008.
- [32] F. Giannetti and P. Luchini, “Structural sensitivity of the first instability of the cylinder wake,” *Journal of Fluid Mechanics*, vol. 581, 167–197, 2007.

- [33] O. Marquet, D. Sipp, and L. Jacquin, “Sensitivity analysis and passive control of cylinder flow,” *Journal of Fluid Mechanics*, vol. 615, pp. 221–252, 2008.
- [34] F. Szodrai, “Quantitative analysis of drag reduction methods for blunt shaped automobiles,” *Applied Science*, vol. 10, p. 4313, 2020.
- [35] S. Alben, M. Shelley, and J. Zhang, “Drag reduction through self-similar bending of a flexible body,” *Nature*, no. 420, p. 479, 2002.
- [36] D. L. Harder, O. Speck, C. L. Hurd, and T. Speck, “Reconfiguration as a Prerequisite for Survival in Highly Unstable Flow-Dominated Habitats,” *Journal of Plant Growth Regulation*, vol. 23, no. 2, pp. 98–107, 2004.
- [37] X. Zhang and H. Nepf, “Flow-induced reconfiguration of aquatic plants, including the impact of leaf sheltering,” *Limnology and Oceanography*, vol. 65, no. 11, pp. 2697–2712, 2020.
- [38] S. Vogel, “Drag and Reconfiguration of Broad Leaves in High Winds,” *Journal of Experimental Botany*, vol. 40, no. 8, pp. 941–948, 1989.
- [39] F. Gosselin, E. De Langre, and B. A. Machado-Almeida, “Drag reduction of flexible plates by reconfiguration,” *Journal of Fluid Mechanics*, vol. 650, pp. 319–341, 2010.
- [40] J. Mosiężny, B. Ziegler, P. Grzymisławski, and R. Ślęfarski, “Base drag reduction concept for commercial road vehicles,” *Energy*, vol. 205, 2020.
- [41] M. Lorite-Díez, J. Jiménez-González, L. Pastur, O. Cadot, and C. Martínez-Bazán, “Drag reduction on a three-dimensional blunt body with different rear cavities under cross-wind conditions,” *Journal of Wind Engineering and Industrial Aerodynamics*, vol. 200, p. 104 145, 2020.
- [42] G. Bonnavion and O. Cadot, “Boat-tail effects on the global wake dynamics of a flat-backed body with rectangular section,” *Journal of Fluids and Structures*, vol. 89, pp. 61–71, 2019.
- [43] M. M. Zdravkovich, “Review and classification of various aerodynamic and hydrodynamics means for suppressing vortex shedding,” *Journal of Wind Engineering and Industrial Aerodynamics*, vol. 7, pp. 145–189, 1981.
- [44] E. Sanmiguel-Rojas, J. I. Jiménez-González, P. Bohorquez, G. Pawlak, and C. Martínez-Bazán, “Effect of base cavities on the stability of the wake behind slender blunt-based axisymmetric bodies,” *Physics of Fluids*, vol. 23, no. 11, p. 114 103, 2011.
- [45] C. Othmer, “Adjoint methods for car aerodynamics,” *Journal of Mathematics in Industry*, vol. 4, no. 1, pp. 1–23, 2014.
- [46] P. Meliga, O. Cadot, and E. Serre, “Experimental and theoretical sensitivity analysis of turbulent flow past a square cylinder,” *Flow, Turbulence and Combustion*, vol. 97, 4 2016.
- [47] L. Gardell, “Low drag truck cabs,” 1980.
- [48] A. D’Hooge, R. Palin, L. Rebbeck, J. Gargoloff, and B. Duncan, “Alternative simulation methods for assessing aerodynamic drag in realistic crosswind,” *SAE International Journal of Passenger Cars - Mechanical Systems*, vol. 7, 2 2014.
- [49] J. M. G. De la Cruz, A. R. Oxlade, and J. F. Morrison, “Passive control of base pressure on an axisymmetric blunt body using a perimetric slit,” *Physical Review Fluids*, vol. 2, 4 2017.

- [50] G. Bonnavion and O. Cadot, “Unstable wake dynamics of rectangular flat-backed bluff bodies with inclination and ground proximity,” *Journal of Fluid Mechanics*, vol. 854, 2018.
- [51] L. Liu, Y. Sun, X. Chi, G. Du, and M. Wang, “Transient aerodynamic characteristics of vans overtaking in crosswinds,” *Journal of Wind Engineering & Industrial Aerodynamics*, vol. 170, pp. 46–55, 2017.
- [52] C. Covaci and A. Gontean, “Piezoelectric energy harvesting solutions: A review,” *Sensors (Switzerland)*, vol. 20, 12 2020.
- [53] A. Abdelkefi, “Aeroelastic energy harvesting: A review,” *International Journal of Engineering Science*, vol. 100, 2016.
- [54] M. Zhou, Q. Chen, Z. Xu, and W. Wang, “Piezoelectric wind energy harvesting device based on the inverted cantilever beam with leaf-inspired extensions,” *AIP Advances*, vol. 9, 3 2019.
- [55] G. D. Nayer, A. Kalmbach, M. Breuer, S. Sicklinger, and R. Wuchner, “Flow past a cylinder with a flexible splitter plate: A complementary experimental-numerical investigation and a new fsi test case (fsi-pfs-1a),” *Computers & Fluids*, vol. 99, pp. 18–43, 2014.
- [56] R. Abdi, N. Rezazadeh, and M. Abdi, “Investigation of passive oscillations of flexible splitter plates attached to a circular cylinder,” *Journal of Fluids and Structures*, vol. 84, pp. 302–317, 2019.
- [57] T. R. Sahu, M. Furquan, and S. Mittal, “Numerical study of flow-induced vibration of a circular cylinder with attached flexible splitter plate at low Re ,” *Journal of Fluid Mechanics*, vol. 880, 551–593, 2019.
- [58] E. Binyet, C. Y. Huang, and J. Y. Chang, “Characterization of a vortex-induced vibrating thin plate energy harvester with particle image velocimetry,” *Microsystem Technologies*, vol. 24, no. 11, pp. 4569–4576, 2018.
- [59] C. Marais, B. Thiria, J. E. Wesfreid, and R. Godoy-Diana, “Stabilizing effect of flexibility in the wake of a flapping foil,” *Journal of Fluid Mechanics*, vol. 710, 2012.
- [60] S. Shukla, R. Govardhan, and J. Arakeri, “Dynamics of a flexible splitter plate in the wake of a circular cylinder,” *Journal of Fluids and Structures*, vol. 41, pp. 127–134, 2013, Special issue on Bluff Body Flows (Blubof2011).
- [61] J. Lee and D. You, “Study of vortex-shedding-induced vibration of a flexible splitter plate behind a cylinder,” *Physics of Fluids*, vol. 25, p. 110 811, 2013.
- [62] W. Dettmer and D. Peric, “A computational framework for fluid-structure interaction: Finite element formulation and applications,” *Computer Methods in Applied Mechanics and Engineering*, vol. 195, pp. 5754–5779, 2006.
- [63] M. Furquan and S. Mittal, “Flow past two square cylinders with flexible splitter plates,” *Computational Mechanics*, vol. 55, no. 6, pp. 1155–1166, 2015.
- [64] K. R. Sharma and S. Dutta, “Flow control over a square cylinder using attached rigid and flexible splitter plate at intermediate flow regime,” *Physics of Fluids*, vol. 32, no. 1, p. 014 104, 2020.
- [65] J. Wu, Y. L. Qiu, C. Shu, and N. Zhao, “Flow control of a circular cylinder by using an attached flexible filament,” *Physics of Fluids*, vol. 26, no. 10, p. 103 601, 2014.

- [66] F. Fish and G. Lauder, “Passive and active flow control by swimming fishes and mammals,” *Annual Review of Fluid Mechanics*, vol. 38, no. 1, pp. 193–224, 2006.
- [67] H. Choi, H. Park, W. Sagong, and S. Lee, “Biomimetic flow control based on morphological features of living creatures,” *Physics of Fluids*, vol. 24, no. 12, p. 121302, 2012.
- [68] E. de Langre, “Effects of wind on plants,” *Annual Review of Fluid Mechanics*, vol. 40, 2008.
- [69] N. Mazellier, A. Feuvrier, and A. Kourta, “Biomimetic bluff body drag reduction by self-adaptive porous flaps,” *Comptes Rendus Mecanique*, vol. 340, no. 1, pp. 81–94, 2012.
- [70] D. Kim, H. Lee, W. Yi, and H. Choi, “A bio-inspired device for drag reduction on a three-dimensional model vehicle,” *Bioinspiration & Biomimetics*, vol. 11, no. 2, p. 026004, 2016.
- [71] K. R. Sharma and S. Dutta, “Flow control over a square cylinder using attached rigid and flexible splitter plate at intermediate flow regime,” *Physics of Fluids*, vol. 32, 1 2020.
- [72] S. Vogel, “Drag and flexibility in sessile organisms,” *American Zoologist*, vol. 24, no. 1, pp. 37–44, 1984.
- [73] S. Satheesh and F. J. Huera-Huarte, “On the drag reconfiguration of plates near the free surface,” *Physics of Fluids*, vol. 31, no. 6, p. 067106, 2019.
- [74] F. P. Gosselin and E. de Langre, “Drag reduction by reconfiguration of a poroelastic system,” *Journal of Fluids and Structures*, vol. 27, no. 7, pp. 1111–1123, 2011.
- [75] Y. Jin, J. T. Kim, S. Cheng, O. Barry, and L. P. Chamorro, “On the distinct drag, reconfiguration and wake of perforated structures,” *Journal of Fluid Mechanics*, vol. 890, A1, 2020.
- [76] M. J. Shelley and J. Zhang, “Flapping and bending bodies interacting with fluid flows,” *Annual Review of Fluid Mechanics*, vol. 43, no. 1, pp. 449–465, 2011.
- [77] E. de Langre, A. Gutierrez, and J. Cossé, “On the scaling of drag reduction by reconfiguration in plants,” *Comptes Rendus Mecanique*, vol. 340, no. 1, pp. 35–40, 2012.
- [78] A. Bhati, R. Sawanni, K. Kulkarni, and R. Bhardwaj, “Role of skin friction drag during flow-induced reconfiguration of a flexible thin plate,” *Journal of Fluids and Structures*, vol. 77, pp. 134–150, 2018.
- [79] “Numerical analysis of the flow-induced vibrations in the laminar wake behind a blunt body with rear flexible cavities,” *Journal of Fluids and Structures*, vol. 100, p. 103194, 2021.
- [80] G. Assi, P. W. Bearman, and N. Kitney, “Low drag solutions for suppressing vortex-induced vibration of circular cylinders,” *Journal of Fluids and Structures*, vol. 25, pp. 666–675, 2009.
- [81] F. Gu, J. S. Wang, X. Q. Qiao, and Z. Huang, “Pressure distribution, fluctuating forces and vortex shedding behavior of circular cylinder with rotatable splitter plates,” *Journal of Fluids and Structures*, vol. 28, 2012.

- [82] A. Feuvrier, N. Mazellier, and A. Kourta, "Self-adaptive control of a bluff body wake by means of porous flaps," *International Journal of Engineering Systems Modelling and Simulation*, vol. 5, 1-3 2013.
- [83] J. I. Jiménez-González and F. J. Huera-Huarte, "Experimental sensitivity of vortex-induced vibrations to localized wake perturbations," *Journal of Fluids and Structures*, vol. 74, 2017.
- [84] J. I. Jiménez-González, C. García-Baena, J. F. Aceituno, and C. Martínez-Bazán, "Flow-induced vibrations of a hinged cavity at the rear of a blunt-based body subject to laminar flow," *Journal of Sound and Vibration*, vol. 495, 2021.
- [85] M. H. Dickinson, C. T. Farley, R. J. Full, M. A. Koehl, R. Kram, and S. Lehman, "How animals move: An integrative view," *Science*, vol. 288, 2000.
- [86] J. O. Dabiri, S. P. Colin, J. H. Costello, and M. Gharib, "Flow patterns generated by oblate medusan jellyfish: Field measurements and laboratory analyses," *Journal of Experimental Biology*, vol. 208, 2005.
- [87] A. Hedenström, "How insect flight steering muscles work," *PLoS Biology*, vol. 12, 3 2014.
- [88] A. J. Bergou, S. Xu, and Z. J. Wang, "Passive wing pitch reversal in insect flight," *Journal of Fluid Mechanics*, vol. 591, 2007.
- [89] R. Dudley, "The biomechanics of insect flight: Form, function, evolution," *Annals of the Entomological Society of America*, vol. 93, 2000.
- [90] M. S. Triantafyllou, G. S. Triantafyllou, and D. K. Yue, "Hydrodynamics of fishlike swimming," *Annual Review of Fluid Mechanics*, vol. 32, 2000.
- [91] G. K. Taylor, R. L. Nudds, and A. L. Thomas, "Flying and swimming animals cruise at a strouhal number tuned for high power efficiency," *Nature*, vol. 425, 2003.
- [92] N. Vandenbergh, J. Zhang, and S. Childress, "Symmetry breaking leads to forward flapping flight," *Journal of Fluid Mechanics*, vol. 506, 2004.
- [93] R. Godoy-Diana, C. Marais, J. L. Aider, and J. E. Wesfreid, "A model for the symmetry breaking of the reverse Bénard-von Kármán vortex street produced by a flapping foil," *Journal of Fluid Mechanics*, vol. 622, 2009.
- [94] R. J. Bomphrey and R. Godoy-Diana, "Insect and insect-inspired aerodynamics: Unsteadiness, structural mechanics and flight control," *Current Opinion in Insect Science*, vol. 30, 2018.
- [95] D. A. Grimaldi and M. S. Engel, *Evolution of the Insects*. Cambridge University Press, Cambridge [U.K.] ; New York, 2005.
- [96] R. Wootton, "The geometry and mechanics of insect wing deformations in flight: A modelling approach," *Insects*, vol. 11, 7 2020.
- [97] R. Godoy-Diana, J. L. Aider, and J. E. Wesfreid, "Transitions in the wake of a flapping foil," *Physical Review E - Statistical, Nonlinear, and Soft Matter Physics*, vol. 77, 1 2008.
- [98] S. Ramanarivo, R. Godoy-Diana, and B. Thiria, "Rather than resonance, flapping wing flyers may play on aerodynamics to improve performance," *Proceedings of the National Academy of Sciences of the United States of America*, vol. 108, 15 2011.

- [99] B. Thiria and R. Godoy-Diana, “How wing compliance drives the efficiency of self-propelled flapping flyers,” *Physical Review E - Statistical, Nonlinear, and Soft Matter Physics*, vol. 82, 1 2010.
- [100] S. Michelin and S. G. Llewellyn Smith, “Resonance and propulsion performance of a heaving flexible wing,” *Physics of Fluids*, vol. 21, 7 2009.
- [101] R. Antier, “Des plis et des ailes, de l’étude d’un pli simple au renforcement d’ailes battantes bio-inspirées,” Ph.D. dissertation, PMMH, Université de Paris, 2021.
- [102] E. I. Fontaine, F. Zabala, M. H. Dickinson, and J. W. Burdick, “Wing and body motion during flight initiation in drosophila revealed by automated visual tracking,” *Journal of Experimental Biology*, vol. 212, 9 2009.
- [103] R. B. Srygley and A. L. Thomas, “The aerodynamics of hovering insect flight. vi. lift and power requirements,” *Philosophical Transactions of the Royal Society of London. B, Biological Sciences*, vol. 305, 1122 1984.
- [104] R. B. Srygley and A. L. Thomas, “Unconventional lift-generating mechanisms in free-flying butterflies,” *Nature*, vol. 420, 6916 2002.
- [105] M. H. Dickinson, F. O. Lehmann, and K. G. Götz, “The active control of wing rotation by *Drosophila*,” *The Journal of experimental biology*, vol. 182, 1993.
- [106] A. M. Mountcastle and T. L. Daniel, “Aerodynamic and functional consequences of wing compliance,” *Experiments in Fluids*, vol. 46, 5 2009.
- [107] C. P. Ellington, “The aerodynamics of hovering insect flight. v. a vortex theory,” *Philosophical Transactions of the Royal Society of London. B, Biological Sciences*, vol. 305, 1122 1984.
- [108] M. K. Salcedo, J. Hoffmann, S. Donoughe, and L. Mahadevan, “Computational analysis of size, shape and structure of insect wings,” *Biology Open*, vol. 8, 10 2019.
- [109] C. V. D. Berg and C. P. Ellington, “The three-dimensional leading-edge vortex of a ‘hovering’ model hawkmoth,” *Philosophical Transactions of the Royal Society B: Biological Sciences*, vol. 352, 1351 1997.
- [110] R. J. Wootton, “Support and deformability in insect wings,” *Journal of Zoology*, vol. 193, 4 1981.
- [111] Robin J. Wootton, “Function, homology and terminology in insect wings,” *Systematic Entomology*, vol. 4, 1 1979.
- [112] S. M. Walker, A. L. Thomas, and G. K. Taylor, “Deformable wing kinematics in free-flying hoverflies,” *Journal of the Royal Society Interface*, vol. 7, 42 2009.
- [113] P. Wu, P. Ifju, and B. Stanford, “Flapping wing structural deformation and thrust correlation study with flexible membrane wings,” *AIAA Journal*, vol. 48, 9 2010.
- [114] T. Nakata and H. Liu, “Aerodynamic performance of a hovering hawkmoth with flexible wings: A computational approach,” *Proceedings of the Royal Society B: Biological Sciences*, vol. 279, 1729 2012.
- [115] R. Godoy-Diana, R. Antier, C. García-Baena, *et al.*, “Insect-inspired two-vein flapping wings with anisotropic rigidity,” in *APS March Meeting 2022 (Chicago, US, March 2022)*, Chicago, US, 2022.
- [116] G. de Croon, M. Percin, B. Remes, R. Ruijsink, and C. D. Wagter, *The DelFly*. 2016.

- [117] T. L. Hedrick, "Software techniques for two and three-dimensional kinematic measurements of biological and biomimetic systems," *Bioinspiration and Biomimetics*, vol. 3, 3 2008.